Master of Science dissertation:

Activity Quantification of Yttrium-90: PET as compared to Bremsstrahlung SPECT

Christian Andersson

Supervisors: Michael Ljungberg and Cecilia Hindorf

Department of Medical Radiation Physics,

Clinical Sciences, Lund

Lund University, Sweden, 2012

Abstract

Introduction: Cancer treatment is a process with continuous development. The most common treatment, within the field of radiation physics, is external radiation therapy, whereas one of the least common methods is Selective Internal RadioTherapy (SIRT). SIRT is a rather novel method for treating liver carcinoma. Microspheres containing ^{90}Y are infused directly into the liver, via the hepatic artery.

Seventeen SIRT-treatments have been performed at Skåne University Hospital (SUS) in Lund since the start in December 2010 until today (June 2012).

Due to the work of David Minarik, the activity distribution is today quantified post-treatment in clinical routine with the single photon emission computed tomography camera (SPECT) system. However, recent work performed by Lhommel et. al has shown the ability to use the positron emission tomography (PET) system to create PET-images with ^{90}Y labeled SIR-spheres. Due to the better spatial resolution in the PET-camera, compared to the SPECT-camera, it is of interest to investigate the possibility to use PET instead of SPECT, for activity quantification of SIRT-patients´ liver. A system with a better spatial resolution has the potential to create a more accurate absorbed dose map from the activity distribution within the liver, compared to the SPECT based system used today.

The aim of this thesis is to evaluate whether PET can be used for activity quantification after ^{90}Y microsphere treatments. Once the most suitable camera is chosen, absorbed dose calculation can be performed with the outcome from the activity distribution shown on the PET- or SPECT -images of the liver.

Materials and methods: For this project, three patients have been treated with SIRT and imaged in both the PET- and SPECT-camera. Furthermore, phantom measurements have been performed both with ^{18}F and ^{90}Y.

Results: For all three patients the PET system overestimates the total activity in the liver with about 20%. The SPECT systems result vary between 0% to – 15% compared to the true activity within the liver. However, more corrections are required on the PET-images to be certain that extra counts originating from the crystals within the PET cameras detector, does not contaminate the image with background noise, and thus giving an overestimation in activity quantification of about 20%.

Conclusion: The results indicate that it is possible to use PET to determine the activity distribution within the liver for patients treated with SIRT. However, further investigations are needed to determine whether PET should replace SPECT.

Populärvetenskaplig beskrivning

En av behandlingsmetoderna mot tumörer i levern på Lunds Universitetssjukhus är SIRT som står för ”Selective Internal RadioTherapy” det vill säga en intern radioterapeutisk behandling, i detta fall specifikt för levern. Behandlingen är cirka tio år gammal och i Lund har den utförts sedan december 2010. Under våren 2012 behandlades tre patienter med SIRT då de inte kan få sina cancertumörer i levern bortopererade av olika skäl. Ofta är det tumörerna metastaserade från en primärtumör i tjocktarmen och som spridit sig och bildat ett blodrikt område vilket därför omöjliggör operation. Även metastaser från primära bröstcancertumörer samt andra endokrina tumörer kan sätta sig i levern. De tumörformer som gagnas av SIRT-behandling är de med en välutvecklad blodförsörjning med många kärl. Det som utnyttjas är det faktum att tumörer (> 20mm diameter) har en blodförsörjning som till minst 80% kommer från leverartären. Detta till skillnad från normal levervävnad som har sin huvudsakliga blodförsörjning från portavenen. Mikroskopiska sfärer (mikrosfärer) innehållande det radioaktiva ämnet Yttrium-90 (^{90}Y) kan då embolisera tumörernas blodförsörjningskanaler. Beta partiklarna emitterade från ^{90}Y sönderfallet kan då på grund av sin förhållandevis långa räckvidd deponera energi i tumörerna. Behandlingen utförs med växelvisa infusioner av mikrosfärer, vatten och kontrastvätska. Först kontrollerar man så att flödet är normalt med kontrastvätska. Sedan administreras SIR-sfärer genom en kateter placerad intraarteriellt vid levern. Därefter fyller man på med vatten för att tömma kateterslangen och slutligen ger man åter kontrastvätska för att kontrollera att flödet ser normalt ut för vidare infusion.
Målet med detta projekt var att absolutbestämma den aktivitet av ^{90}Y som man deponerar i levern för att slå ut cancern. Fördelningen av radioaktivitet i levern mäter man idag genom en tomografisk undersökning (SPECT) dagen efter SIRT behandlingen. Syftet var då att undersöka möjligheten att kvantifiera aktiviteten även med en sk PET-kamera. Detta system mäter fotoner annihilerade från en beta plus partikel (positron). Detta är möjligt då det i 32 sönderfall per en miljon emitteras en positron från ^{90}Y. Denna positron växelverkar med en elektron med en annihilation och efterföljande emission av två motsattriktade fotoner. En PET-kamera är dedicerad att detektera koincidenser från dessa två fotoner med en hög noggrannhet. Frågeställningen var då om det är tilläcklig noggrannhet för att kunna aktivitetskvantifiera ^{90}Y i levern. Frågan var också om PET-systemet är mer lämpat än det nuvarande SPECT-system beträffande denna mätning på grund av PET-systemets bättre upplösningsförmåga jämfört med SPECT. Då skulle detta system ge en mer korrekt bild av den absorberade dosen över levern.
Resultaten visade att fördelningen av aktivitet var mer välbestämd med ett PET system än motsvarande undersökning med SPECT, detta beror sannolikt på att PET systemet har en bättre spatiell upplösning jämfört med SPECT. Dock fanns det i PET bilderna ett bakgrundsbidrag av händelser orsakade av naturlig radioaktivitet i själva detektormaterialet på PET systemet och som bör korrigeras för innan man med säkerhet kan säga hur kvantitativt noga PET bilderna

egentligen är.
För de tre SIRT-patienterna i denna undersökning så visade resultaten att aktiviteten av ^{90}Y överskattas med cirka 20% när man mäter i PET kameran. Motsvarande för SPECT visade ett intervall mellan 0 och 15%, detta jämfört med den sanna framräknade aktiviteten. Med andra ord så visade SPECT på en större säkerhet vad beträffar bestämning av den totala ^{90}Y aktiviteten som administrerats i levern.

Contents

1. Introduction

This project is about accurate activity quantification. Quantification is the term that answers the question: how much? In this project the answer is given in Becquerel (Bq) or Bq per milliliter (ml), the latter meaning activity concentration. When measuring radioactivity in a camera system it is of great concern that the reconstructed activity matches the true activity or activity concentration. The best way to test the system's quantification accuracy is to perform phantom measurements with known activity concentrations or a known total activity. The measured versus true activity is in turn compared and presented as a quotient:

$$\frac{measured\ activity}{true\ activity} = activity\ ratio \quad (1)$$

Further on, accurate activity quantification is necessary in order to perform a correct absorbed dose calculation, both locally and for a total absorbed dose within an organ.

For patients with inoperable liver cancer treated with selective internal radiotherapy (SIRT) due to their inoperable liver cancer, activity quantification as well as activity localization is of great interest.
Today SPECT imaging is performed one day after the operation and infusion of ^{90}Yttrium (^{90}Y) labelled microspheres. The bremsstrahlung spectrum is analysed and an activity distribution can be calculated.

An interesting alternative to SPECT bremsstrahlung imaging, is to use Positron emission tomography (PET). This is performed by imaging annihilation photons emitted from the 32 ppm of the decays from the ^{90}Y that result in an emission of a positron. If sufficient number of positrons from the ^{90}Y is registered as a true coincidence, an image can be created.

PET is widely used to localize tumours because of high contrast and high spatial resolution. The contrast property is utilized when searching for tumours in a patient and is measured in standardized uptake ratio (SUV). SUV is the concentration in a tumour normalized to the total administered activity per body weight (assuming that weight is represented by the volume).
Novel work performed by Lhommel et. al [1, 2] has shown the ability to use the PET -system to create images with ^{90}Y labelled SIR-spheres.

Image quality is important when comparing the PET and SPECT system. Contrast, spatial resolution and system sensitivity are parameters important for the image which is about to be analysed. A poor spatial resolution can lead to misplacement and spread out of counts from the radioactivity imaged, and an insufficient contrast can make the uptake areas difficult to visualize relative the background. Which of the two camera systems, PET or SPECT, that creates the most accurate activity quantification of ^{90}Y is yet to be determined.

2. Background

When irradiating ^{89}Yttrium with neutrons the isotope ^{90}Y can be created. Figure 1 shows the decay scheme [3].

^{90}Y mainly decays by beta emission but has also a minor decay to the first excited state of ^{90}Zirconium resulting in an emission of a positron with maximum energy of 1.78 MeV and mean energy of 0.7 MeV. When the kinetic energy of this positron has been transferred to surrounding material the positron annihilates with a nearby electron resulting in an emission of two photons each with the energy of 511 keV. These are emitted in opposite directions in order to conserve momentum. Since the distribution of the two photon pairs are isotropic, only a small number of these photons will be possible to detect with the PET camera detectors. When the photons are not attenuated along their path, they can be detected generating an event called a "true coincidence". A coincidence is simply a simultaneous detection by two detectors within a time window sufficiently small in order to discriminate other photons not coming from the same annihilation process.

The abundance of the beta plus decay from ^{90}Y occurs only in about 32 cases out of one million [4].

Because of its beta minus emission, ^{90}Y is mainly used for radionuclide therapy, resulting in high energy electrons that can cause a therapeutical absorbed dose for a carcinoma tumour. The maximum and average energy for this electron is 2.27 MeV and 0.9337 MeV, respectively [5]. The average path length is calculated to be 4.0 mm, for soft tissue using data from the National Institute of Standards and Technology (NIST) [6].

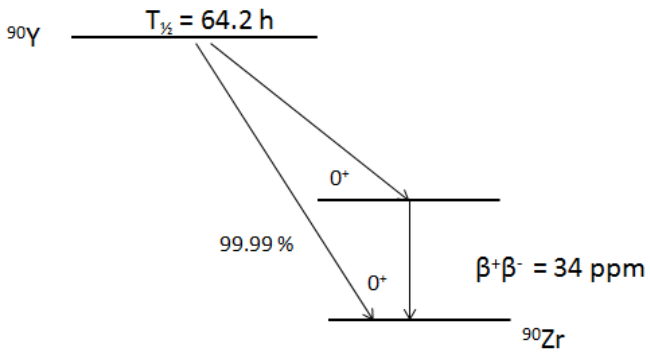

Figure 1. Decay scheme of the ^{90}Y decay. Redrawn from reference [3].

In the Single Photon Emission Computed Tomography (SPECT) it is bremsstrahlung photons from the ^{90}Y that are detected. This is possible since the electrons coming from the beta minus decay from ^{90}Y interact with the strong coulomb field around an atomic nucleus which causes the electron to change its direction, thus causing

the emission of a bremsstrahlung photon. These photons are detected in the SPECT camera´s detector crystal. SPECT is the currently used imaging method after SIRT-treatment. To quantify the continuous bremsstrahlung spectrum with SPECT a lot of corrections are needed, since no clear photo peak exists within this beta spectrum. The photons coming from the ^{90}Y bremsstrahlung production has an energy range up to 2.27 MeV which builds up the spectrum with wanted, but mostly unwanted photons in each energy channel. The correction methods necessary for quantification are many and the result is not easily gained. All methods are thoroughly described in the thesis of David Minarik [7] and will not be discussed further, except for a short summary in the "activity quantification" section below.

Both the PET and the SPECT camera reconstruct images with ordered subset expectation maximization (OSEM). The basic of OSEM is as follows [7]:

- An initial image guess is created, usually a flat matrix
- The initial guess is then projected to sinograms
- The measured projection is compared with the initial guess sinogram
- The comparison creates an error sinogram, which is backprojected
- The initial image is updated with the backprojected error image

This process goes on until a satisfying image is reached, or when the difference between the measured and calculated projection sinogram is sufficiently small.

2.1 Purpose

The main purpose of this work is to evaluate the ability to accurately quantify activity uptake *in vivo*, which is in a patient, with a clinical PET system using both ^{18}Fluorine (^{18}F) and ^{90}Y. In order to establish the accuracy in quantification of ^{90}Y, SIR-spheres labelled with ^{90}Y were used. Tests were performed to evaluate the advantages and disadvantages using these two radio nuclides. ^{18}F was selected as the reference radionuclide since it is the most widely used radionuclide.
In order to be familiar with the system some of the common image quality tests of the PET-camera were performed.

Factors of great importance in the comparison between these two camera systems are; image contrast, spatial resolution, sensitivity and the ability to quantify activity. The latter is of great importance and also in focus of this thesis. The aim was thus to evaluate the activity quantification and compare the results from PET and SPECT measurements, with the purpose of finding which of the two methods is the most accurate in quantification and which is the best system in regards to practical use.

2.3 Introduction to the SIRT treatment

Radio-embolization with microspheres attached with ^{90}Y radionuclides is an increasingly used method for treating un-resectable liver carcinoma. The treatment has been used for about two years at the Skåne University Hospital in Lund and the overall application has been used for about ten years worldwide.

There is a large difference in the blood supply when comparing normal liver tissue with tumours in the liver. Tumours with a diameter larger than 20 mm has its main blood supply originated mostly from the hepatic artery, while normal liver tissue has its blood supply maintained by the portal vein [8]. Therefore, the radioactive spheres are administered directly in the hepatic artery and not the portal vein for the purpose of sparing the normal tissue against unnecessary radiation and absorbed dose. The small microspheres become permanently trapped in the vascular tree that supplies the tumours with blood and thereby giving a high local absorbed dose to the tumour over a long period (determined by the physical half-life of the radionuclide).

Prior to the ^{90}Y SIRT-treatment the administration of ^{99m}Tecnetium labelled macroaggregated albumin (^{99m}Tc-MAA) is required. This is performed in order to create an individual activity administration plan for the patient with respect to the possibility of failure location for the SIR-spheres. The administration of ^{99m}Tc-MAA is performed in the same manner as the upcoming SIRT-treatment with SIR-spheres. The ^{99m}Tc -MAA particles have a range in size between 10-100 µm [9] which is in the same order as the SIR-spheres. Within this pre-treatment operation, coiling against possible pathways for the microspheres is performed. This is in order to evaluate and quantify possible shunting of ^{90}Y particles from the liver into the lungs, but also to determine the blood reflux to nearby endocrine organs [10]. The coiling procedure is then clinically verified with a ^{99m}Tc-MAA injection along with planar gamma camera imaging. The number of counts registered in a region of interest (ROI) over the right and the left lung are calculated and taken into consideration in the treatment plan. The result from this operation is taken into consideration for the upcoming treatment planning, which will be discussed more in “Absorbed dose determination”.

After the infusion of the ^{90}Y labelled spheres, a SPECT imaging is routinely performed, with the purpose of determining the distribution of the activity within the liver, from which there is a possibility to perform an absorbed dose map. Much work on the methods used for activity quantification with the SPECT-camera has been performed in a PhD work by David Minarik, with the main purpose to quantify ^{90}Y SPECT images. This work has led to the possibility of quantifying bremsstrahlung images from SPECT.

2.3.1 The characteristics of SIR-spheres

The small spheres attached with ^{90}Y are available in two different models as presented in table 1 below. Only the SIR-spheres are available in Lund at the moment.

Table 1. Comparison properties of resin spheres and glass spheres [11].

Parameter	Resin	Glass
Trade name	SIR-Spheres	TheraSpheres
Manufacturer and location	Sirtex Medical, Lane Cove, Australia	MDS Nordion, Ottawa, Canada
Diameter	20-60 µm	20-30 µm
Activity per particle	50 Bq	2 500 Bq
Number of microspheres per 3-GBq vial	40-80 x 10^6	1.2 x 10^6
Material	Resin with bound ^{90}Y	Glass with ^{90}Y in matrix

2.3.2 Determination of administered activity

The "Body surface area" (BSA) is a parameter that forms the base for the treatment planning method used at the Skåne University Hospital in Lund. BSA is calculated from the following equation [12]:

$$BSA = 0.20247 \cdot height^{\,0.725} \cdot weight^{0.425} \quad (2)$$

and where *BSA* is in units of m^2, *height* is in units of meter and *weight* is in units of kilograms.

The following equation is used in order to determine the amount of ^{90}Y activity that needs to be administered into the liver:

$$A_{BSA}\,(GBq) = BSA - 0.2 + \left(\frac{tumour\ volume}{tumour\ volume + normal\ liver\ tissue\ volume}\right) \quad (3)$$

Activity reduction is performed after evaluating the planar ^{99m}Tc-MAA-images. Depending on the number of counts in a region of interest (ROI) over the lungs, relative to the counts on a ROI over the liver, the ^{90}Y activity may be decreased by some factor k_{shunt}. For example: if the shunting to the lungs is determined to be less than 10%, then all planned ^{90}Y activity can be administered. If the shunting is larger than 20%, the SIRT treatment will not be completed. Values in between result in a reduction of the planned ^{90}Y activity.

Other factors that can decrease the activity to be administered are:

- Small liver volume
- Powerful pre-treatment chemotherapy
- Large tumour involvement (> 65%)
- Small tumour involvement (< 10%)
- Cirrhosis patients (HCC)

All of the factors above decrease the total administered activity by about 30%. The liver is anatomically divided into two lobes. If only the right lobe is treated the

reduction of activity is 1/3, since this approximately represents the volume given for the left liver lobe. The same procedure applies for the left lobe which is about 1/3 of the total liver volume, which leads to an activity reduction of 2/3 [12].

2.4 Activity Quantification

The evaluation of accurate activity quantification is one of the main purposes of this thesis. During the treatment in Lund, SPECT has been the post-treatment modality clinically applied to get an estimate of the activity distribution within the liver. From these images it is, of course, desirable to predict the outcome of the SIRT treatment by estimating the absorbed dose and relating the tumour response to the absorbed dose. This is, however, not done on a regular basis today. Possible adverse effects as well as tumour to normal liver absorbed dose could also be determined from these images [13]. The spatial resolution is generally better in PET than bremsstrahlung SPECT. Better spatial resolution is one of the main arguments why PET could be a good alternative to SPECT for post-treatment SIRT-patients.

Much work has recently been performed regarding SPECT quantification with ^{90}Y by David Minarik. Since the beta spectrum from a liver containing SIR-spheres is continuous and thus resulting in bremsstrahlung photons with energies from a wide range, the imaging and related activity quantification is not an easy task and is thoroughly discussed in his PhD thesis [7]. Figure 2 shows a spectrum from a phantom measurement with ^{90}Y. The red arrows indicate the energy window used for activity quantification.

A brief explanation of the activity quantification process used for SPECT is required. Initially, the CT image from the SPECT/CT study is scaled from HU to linear attenuation coefficients as a function of photon energies. After this a correction for scatter is performed using the effective source scatter estimation (ESSE) method. The measured image is convolved with a SIMIND produced 3D-kernel representing scatter in the image and then weighted with the density map from the CT scan to compute the effective scatter source. After this the scatter component can be calculated by projecting the effective scatter source [7].

Basically, what is performed in the SPECT bremsstrahlung quantification is simulation of the spectra with Monte Carlo and then subtract what is scattered and unwanted within the specified energy window which is centred at 150 keV with an energy window of 60% [14].

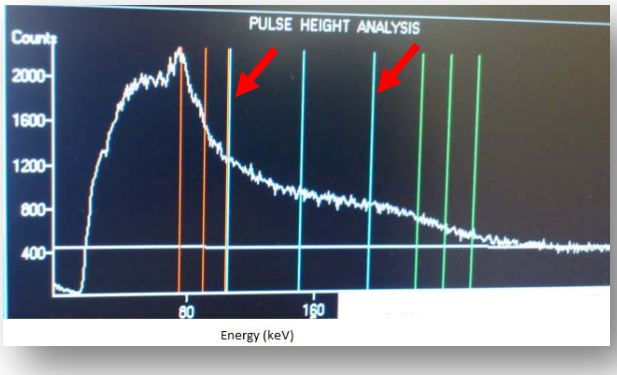

Figure 2. The beta-spectrum produced from the ^{90}Y microspheres within a phantom measurement during this thesis work. The red arrows indicate the energy window used for activity measurement.

The limitation of the PET system and related activity quantification are mostly due to physical phenomena, which show themselves as limiting factors of the spatial resolution. Some of these limitations are stated in the following section.

1) The positrons travel an energy dependent distance with an average of 2.4 mm, in soft tissue, for positrons emitted from ^{18}F and 4.0 mm for positrons emitted from ^{90}Y. This limits the resolution of even the best camera on the market, which is about 5 mm, measured with ^{18}F and performed according to the National Electrical Manufacturers association (NEMA) [15].

2) A limitation in the spatial resolution is the so called “Block effect” -also called the “depth of interaction”. This effect is a parameter coming from the attenuation probabilities lying in the nature of a photon travelling in a medium. A photon has a probability to pass through the initial crystal block and interacting with a crystal next to it. This leads to a misplacement in space and an offset line of response (LOR). This effect is more apparent with off centre annihilations, as visualized in Figure 3. Since the transaxial resolution according to the Discovery PET/CT 690 datasheet [16] is 4.9 mm at 1 cm and 5.5 mm at 10 cm off centre, this effect is most likely small. This since more parameters than the “block effect” is included in this off centre decrease in spatial resolution.

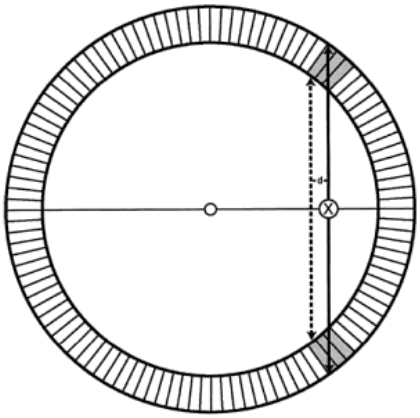

Figure 3. The block effect visualized. The true event is the solid line, which is detected as the dotted line, also called LOR. Image reference [17].

3) Non-collinearity is a degrading factor affecting the systems spatial resolution. It comes from the interacting process where the positron annihilates with an electron and they do not leave each other exactly "back to back" as expected, but instead with a deviation of approximately 0.25 degrees. This is because of residual momentum from the annihilation process [18]. This leads to misplacement dependent on the ring size, a larger ring gives a more pronounced effect. To calculate this deviation in millimeter the formula below can be used:

$$deviation\ (mm) = D \cdot 0.0022, \qquad (4)$$

where D is the ring diameter in the units of millimeter. For an 81 cm detector ring this becomes 810x0.0022 = 1.78 mm.

4) The pixel size is also a limiting factor. A larger matrix size means a smaller pixel size and also a theoretically better spatial resolution. The effect works the other way around on smaller matrix sizes.

The detectors in the PET system also affect the spatial resolution. Some parameters are;

- Detector width
- Stopping power of the material
- Sampling interval between the detectors

3 Material and methods

3.1 The PET/CT camera used in this project

The PET/CT-camera at the Skåne University Hospital in Lund that has been used in the project is a Discovery 690 (General Electric, Milwaukee, USA). Technical details about the PET/CT-system are presented in Table 2 below.

Table 2. PET/CT camera information [15].

Transaxial Field of View with CT attenuation correction	70 cm
Axial Field of View	15.7 cm
Axial Sampling interval	3.27 mm
Number of rings	24
Number of image planes	47
Coincidence window	4.9 ns
Energy window	425-650 keV
Number of Cerium activated Lutetium based crystals per ring	576
Crystal size	4.2 mm x 6.3 mm x 25 mm
Reconstruction time per frame (128x128 matrix)	150 s
Number of CT slices	64
Number of solid state elements for CT	58 368
Rotational time	Variable: 0.35 – 2 s
CT reconstruction matrix	512

3.1.1 Image Reconstruction

Vue Point FX™ is the reconstruction software used in the PET camera system that incorporates information about "time-of-flight" (TOF) in the OSEM algorithm. TOF measures the Δt (s) between the incident annihilation photons and this information is used to create a smaller LOR than the whole FOV diameter. TOF information is dependent on the timing resolution of the PET system. The Discovery 690 has a timing resolution of 500 ps which gives a positioning uncertainty of 7.5 cm as determined by the equation:

$$\Delta x = c\,\Delta t / 2 \qquad (5)$$

where Δt is the positioning uncertainty, Δx is the positioning error and c is the speed of light.

The standard reconstruction protocol uses OSEM with 12 subsets and 3 iterations. The number of iterations and subsets can be increased or decreased post

measurement. The PET-data can also be acquired in list mode, which makes it possible to create other, but only shorter, acquisition times.

3.1.2 Correction methods PET/CT

The raw data which comes out from a measurement needs to be corrected from various physical effects. Necessary corrections for an accurate quantification of the PET-images are: scatter, random, dead-time and photon attenuation. The differences between these effects are described in Figure 4.

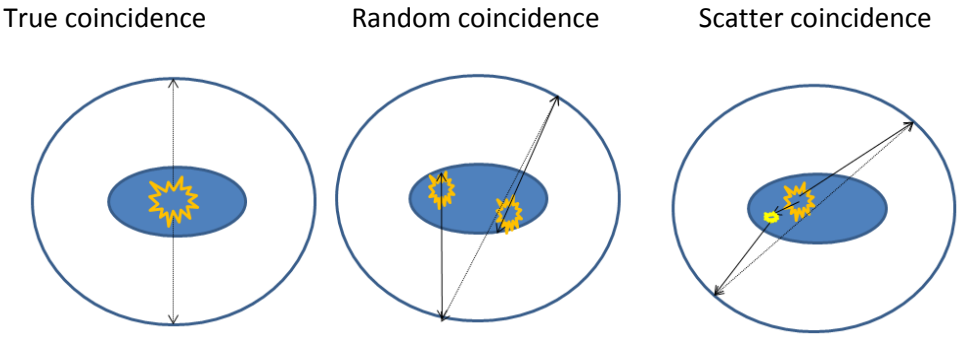

Figure 4. Different coincidences in PET imaging. The yellow star indicates a simulated radioactive source and the small dot in "scatter coincidence" indicates a scattered process. Redrawn from [19] page 192.

Scatter correction: A model based scatter-algorithm is used [20]. Even though it is a rather complex procedure, an attempt to summarize this is performed. The scatter method is a step by step process:
First a transmission information scan is obtained from the CT-scan. Then the PET-acquisition is performed. A normalization procedure is then applied on this PET-acquisition making sure that all detectors remain equal regarding efficiency. Now attenuation correction is performed on the PET-acquisition. After this, scatter correction is performed using a scatter correction model. This model uses a fitting algorithm on the PET-acquisition data to estimate a scatter vector from a scatter tail. The PET-acquisition data is now compared with the scatter vector in order to identify the number of secondary emission data in the PET-acquisition data. At this time many estimated scatter vectors are calculated. The comparison leads to an estimation of secondary emission data. This is now corrected for on the original data, -that is- random coincidences are subtracted from the total prompt and only true coincidences are left [21].

Random correction: "Estimations of Singles" is the method used [22]. This means that the rate of random coincidences per second is estimated with the formula:

$$R_{i,j} = 2\tau S_a S_b \qquad (6)$$

where τ is the timing window of the PET system and S_a/S_b is the number of counts per second for each detector. Since S_a and S_b are approximately the same the equation simplifies to:

$$R_{i,j} = 2\tau S^2 \quad (7)$$

This method assumes no redistribution of the activity [19]. In the case of SIRT treatment no redistribution and no leakage of the SIR-spheres is assumed once embolized in the tumour vessel [23]. Even if a redistribution of these SIR-spheres would occur, it would most likely not be possible to see on the images because it would probably be a slow process compared to the acquisition time.

Attenuation correction: This is performed with the integrated CT in the Discovery 690, which is a 64 slices GE Lightspeed™ VCT[1] with full 3D volumetric reconstruction. An image acquired with the CT creates the attenuation map to correct the PET images with. CT images are measured in Hounsfield Units (HU) which is converted to linear attenuation coefficients. The smaller voxel size in the CT images leads to the need of down sampling to a size matching the PET image matrix size.

Dead time correction: to account for events that may have happened during the data handling of a recent coincidence event this correction is necessary. Depending of which radio nuclide is being measured the correction is more or less pronounced.

Decay correction: A decay correction is automatically performed with the protocol chosen. For ^{90}Y this is a minor problem since the measurement time in the PET or SPECT camera usually is small compared to the half-life of ^{90}Y.

Normalization: In order for all LOR to have the same response a correction is necessary for each detector pair. This correction matrix is a result of a measurement where the same result is expected for all LORs. This normalization correction is necessary since the sensitivity across the FOV has an almost pyramid shaped form, meaning the sensitivity of center decreases compared to the centre, which needs to be compensated for. The normalization for each detector pair is included in the OSEM reconstruction [15].

3.2 The SPECT/CT camera used in this project

The SPECT camera with integrated CT is a General Electric Discovery VH. It consists of detection NaI(Tl)-crystals, which is 2.54 cm thick. When measuring ^{90}Y activity a High Energy General Purpose (HEGP) collimator is chosen in order to minimize the septum penetration from the high energy photons coming from the ^{90}Y bremsstrahlung spectrum.
The energy window used for acquisition was a 60% energy window centred at 150

[1] Volume CT Technology

keV. The energy window then extends from 105-195 keV.
Number of slices for the SPECT camera is 64, and the matrix size is 64x64. This gives a voxel size of about 8x8x8 mm^3. The SPECT acquisition was performed with 60 s per angle and with 60 angles.
The spatial resolution for the SPECT camera is about 16 mm, measured with ^{131}Iodine at 15 cm source to HEGP-collimator distance [7]. The sensitivity for the SPECT/CT system is 1.02 cps /MBq with the HEGP-collimator, measured with ^{90}Y [7].
For attenuation correction purposes the integrated CT was used. The tube voltage was 140 kV and the anode current was 2.5 mAs. Matrix size for the CT images was 128x128 which gave a voxel size of half the one for the SPECT images, which is 4x4x4 mm^3.

3.2.1 Correction methods

Since it is the bremsstrahlung spectrum that is measured, necessary corrections are performed to discriminate the scattered photons. The scattered photons contribution is simulated in computer software named SIMIND[2]. This program can Monte Carlo (MC) simulate the ^{90}Y bremsstrahlung spectrum and thus give an indication of the amount of scattered photons present within the spectrum. After this a subtraction of the scattered photons is performed to obtain what is supposed to be the total number of unscattered photons.
Attenuation correction was performed from the CT image where HU were converted to linear attenuation coefficients.
Corrections and reconstructions were performed using the **LundAdose[3]** software. Also a collimator-detector response correction was performed and included in the reconstruction process. Six subsets and an optional number of iterations were used in the reconstruction algorithm.

3.3 Experimental evaluation

For the evaluation of the information from the PET and SPECT systems an image analysing program was necessary. For this the program AMIDE[4] was chosen. AMIDE is a medical imaging data examiner that can import Dicom files and images, received from the PET and SPECT system. The program fits the needs for analysing the experimental outcome from these measurements very well. Mainly because of the ability to exactly determine the volume of interest (VOI), but also because of the simplicity of applying it on images.

[2] http://www2.msf.lu.se/simind/
[3] http://www.exelisvis.com/network/usecase/detail.asp?l=French&app_id=148
[4] http://amide.sourceforge.net/

^{18}Fluorine Experiments

In order to get a better understanding of the PET-system used at the clinical department at the Skåne University Hospital in Lund, some basic experiments were performed. Various performance tests of the PET system are necessary in order to evaluate the upcoming experimental results.
The phantom used in most measurements was the NEMA body phantom, Figure 5.

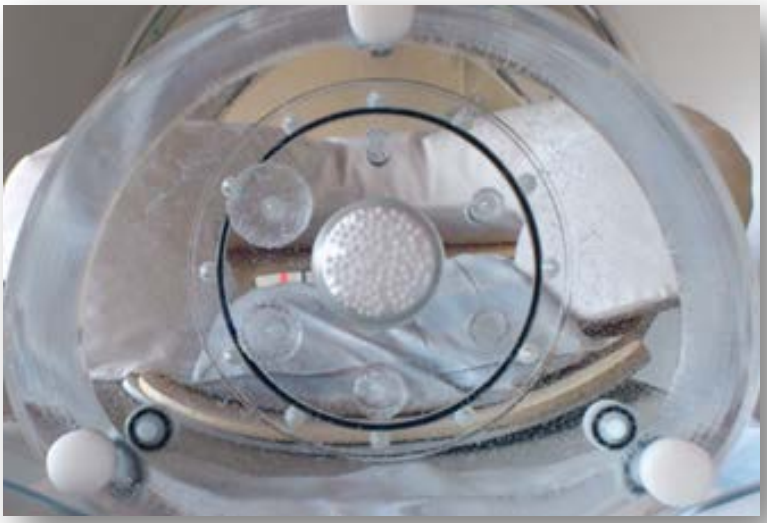

Figure 5. The NEMA body phantom. The different sized spheres surrounding the simulated "lung" volume in the middle of the phantom.

4 Quantification ^{18}Fluorine

A volume of interest (VOI) was created in AMIDE. This VOI was sphere-shaped and virtually placed to surround the spheres in the NEMA body phantom. Additionally 8 mm in diameter was added to the true sphere-size for these VOIs.
The mean activity was noted, and also the volume of the VOI. The total activity is the mean activity concentration multiplied with the volume of interest.
Background subtraction was performed, even though it was very low.
Noteworthy is that this is not a conventional method to quantify activity into a volume. But with the liver in mind, it is decided that this is an applicable method, concerning quantification. This since it is necessary to take into account the partial volume effect (PVE) which spreads out the activity into neighbouring voxels. This method would be more doubtful to apply when creating an absorbed dose map of the liver, since the absorbed dose surrounding the liver could be substantial. But one has to keep in mind that it is not the positrons that give rise to the large absorbed dose, it is the beta minus decay. Electrons from the beta minus decay have an average range of 4.0 mm compared to the average range of the positron,

which is 2.8 mm.
Different number of iterations were compared and plotted. A table showing the relative background noise with increasing number of iterations from a VOI placed away from the hot spheres is shown, table 3. The 100% background noise level is determined from the 3 iteration value.

4.1 Recovery Coefficients for ^{18}Fluorine

A Recovery Coefficient (RC) curve is said to test the PET system´s linear response with respect to different sized spheres when filled with radioactivity [24]. The NEMA body phantom (Figure 1) was used for this test. The RC curve describes the relative deviation from the true value of radioactivity; this is plotted as a function of sphere size.
The ratio of the true activity and the measured activity was plotted. The measurements were evaluated using the AMIDE image processing software, where accurate sized VOIs can be applied. The VOIs were drawn on the CT -image and copied to the PET -image.
The purpose was to compare the geometrical reconstructed activity with the true activity. VOI was made in accordance with the specified diameter for each sphere from the NEMA body phantom.
Reconstructions with different numbers of iteration were also performed, since the clinical settings are 3 iterations and 12 subsets. Included is also a reconstruction without TOF.
A line profile was drawn to compare and visualize the partial volume effect (PVE). Maximum values and 12.5% VOIs were also plotted with different number of iterations. The 12.5% VOI has a sphere shape with the volume equal to 1/8 of the original phantom sphere and chosen since it is an easy VOI to apply on images viewed at the workstation or anywhere else, thus easy to apply clinically. The 12.5% VOI corresponds to a half diameter compared to a full size diameter VOI. Added were also the results from a 70% VOI, since it is also an accepted VOI according to *The Netherlands protocol for standardisation and quantification of FDG whole body PET studies in multi-centre trials* [25].
The maximum value is included since it is simple to apply and proposed by Boellard et al [25].

4.2 Spheres to Background ratio

Similar to the RC measurement described above, measurements with activity in the background and with different activity ratios relative to the spheres were performed. The theoretical and the quantified activity from the images were compared, with different number of iterations. AMIDE was used where VOIs of exact size of the spheres were applied and centred with help from the CT images. The size of the sphere-shaped VOIs to measure background activity were 7 mm in diameter, and the “lung” volume, which is the middle of the NEMA body phantom was used to evaluate the background noise level, and also for subtraction of this. This VOI was 7 mm in diameter as well.

Activity ratios were 7:1, 5:1 and 3:1. The 7:1 ratio was chosen because a large contrast was desirable. The other ratios were chosen because of the assumption

in literature that the tumour to normal liver ratio often is said to be 3:1. The last 5:1 ratio were chosen because it was in-between the other ratios.
Recovery curves and curves showing the reconstructed ratios were performed. Also a summary graph showing standard protocol measurements with the different activity ratios are shown. Furthermore different sized VOIs applied in the non-background case, which is the RC measurement, are presented.

A table presenting the true activity concentration in the background versus the spheres is shown below.

Table 3. Theoretical activity concentrations from the experiments with different activity ratios.

	Spheres	Background
True activity ratio	True activity conc. kBq/ml	True activity conc. kBq/ml
7:1	35.3	5.07
5:1	26.7	5.30
3:1	15.4	5.16

5 Spatial resolution ^{18}Fluorine and ^{90}Yttrium

A spatial resolution measurement was performed. Even though it was not made according to the NEMA protocol, which is the conventional performance measurement approach, it was still applicable since only a relative comparison between ^{18}F and ^{90}Y was desired. Two line-sources, with different diameter, were filled with ^{18}F activity, approximately 100 MBq each. They were placed on a plastic plate, both about 5 cm off axis on each side laterally viewed. On top of them an additional plastic plate was placed to ensure that the positrons emitted from ^{18}F have something to interact with. Figure 6 shows the experimental setup.

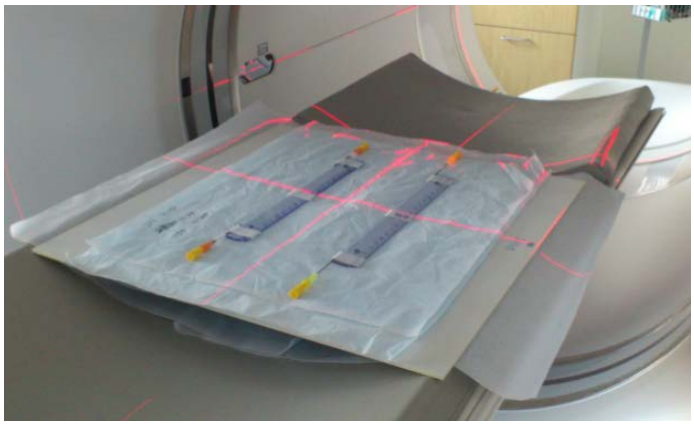

Figure 6. The experimental setup for the spatial resolution measurement with ^{18}F.

The line sources´ inner diameter was about 1.4 mm for the thick line and the thin line source were about half that in size, which is 0.7 mm. The measurement was evaluated in AMIDE where a line profile could be applied and the tangential FWHM were obtained.

The medical physicist employed at the clinical department had recently performed a similar measurement, but with ^{90}Y instead of ^{18}F. These measurements were available for this project and thus could be analysed in the same manner as for ^{18}F. Matrix sizes 192x192 and 256x256 were compared and evaluated.

6 Beta spectrum from ^{32}Phosporus

A simple test to see whether there is any visible differences when reconstructing images with different protocols was made. This was supplemented with the aim to find out whether or not the PET-camera finds any true coincidences from ^{32}P, which is thought to be a pure beta minus emitter. ^{32}P has a very small branch of positrons as well as ^{90}Y. For ^{32}P the positron branch is approximately 0.7 per GBq [26], thus there is a theoretical possibility to find a true coincidence. The purpose of the measurement was also to see if the camera mistakenly adds some counts originating from the bremsstrahlung spectra produced by the beta particles, and if these are detected as a true coincidence. The activity source used was about 40 MBq of ^{32}P. This is a rather low activity to statistically be able to find any true coincidences, but the activity concentration is perhaps sufficient to determine if any bremsstrahlung photons will be detected as annihilation photons. This since the amount of ^{32}P was approximately one tablespoon (15 ml) and no further dilution was performed, this equals an activity concentration of about 3MBq/ml. Protocols used for the measurement were ^{18}F and ^{90}Y, since no protocol existed for ^{32}P.
A plastic sphere was filled with the ^{32}P activity and then placed at the bottom of a larger phantom. This phantom was filled with water and a PET/CT scan was performed. The acquisition time was 20 minutes.
A quick evaluation was performed and this lead to the need for background measurements.

6.1 Background level

As a follow up from the measurement with ^{32}P above, another measurement was performed. To find out if there is any difference between the protocols used; 30 min scans without any phantom (blank scan) with ^{18}F and ^{90}Y protocol were performed. A large VOI was created in AMIDE (200x150x150) and the total activity within this VOI was evaluated. The suspicion is that the background noise level is increased in the ^{90}Y protocol and thus larger than in the ^{18}F protocol, which could possibly be due to the large scale factor because of the small branch of positron decay for ^{90}Y. The background noise level could perhaps determine if the difference in protocols used is a factor of about 30 200, similar to the positron branch ratio between ^{18}F and ^{90}Y.

7 ^{90}Yttrium simulation

Since there was a shortage of ^{90}Y in a major part of the spring, ^{18}F was considered a substitute. The only obstacle was to get the activity representable to the expected number of coincidence photons from ^{90}Y. This since the branch of positrons in ^{18}F is about 30 200 times larger than for ^{90}Y.

In order to evaluate the results in a more quantitative manner it was necessary to reach a realistic activity level. A theoretical assumption was required; an assumption of a liver mass of 1.5 kg and density approximately equal to water gives a volume of 1.5 l. Assuming also an administration of 1.5 GBq, this gives a theoretical number of positrons per seconds of about 32 000 per litre, or in activity concentration 32 Bq/ml, for ^{18}F.

A large activity concentration was left in the NEMA body phantom day 1. The next day, a measurement with protocols for ^{18}F and ^{90}Y was performed separately. The activity concentration of ^{18}F was then very low and calculated to be approximately 30 Bq/ml.

The PET camera makes a correction for the decay in the ^{18}F protocol, but, of course, not the same in the ^{90}Y protocol when measuring ^{18}F. This had to be corrected for, manually with the following calculation.

The time integral from 0 to 20 minutes (PET acquisition time) was calculated, that is;

$$\int_0^{20} \exp\left(-\frac{\ln(2)}{109.8}t\right) dt = 18.79 \tag{8}$$

This shows that the decay not taken into account for is equal to the quotient $\frac{18.79}{20} = 0.94$, which is a 6% decay during the 20 min measurement. The measured values, from the ^{90}Y protocol, were therefore divided by 0.94. The low correction factor already performed from the systems ^{90}Y protocol were 1.00815, which was ignored.

A simulated ^{90}Y activity was calculated from the results from the ^{90}Y protocol measurement. The factor $\frac{967000}{32}$ was multiplied with the true ^{18}F activity. This activity ratio is plotted and the same method is applied on the ^{18}F measurement.

^{90}Yttrium experiments

8 Recovery coefficient ^{90}Yttrium

Measurements with the NEMA body phantom had recently been performed by the physicists at the clinical department at SUS in Lund. About 300 MBq ^{90}Y had been put into the NEMA body phantoms spheres.

A 30 minute PET and SPECT -scan was performed and compared with respect to quantitative results.

Measurements with the phantom were performed over a few weeks, which means that the same phantom measurement but with different activities due to decay were scanned. This was performed until almost no activity was left in the phantom. The results are presented as different activity concentrations and the evaluation is performed in AMIDE with sphere sized VOIs. These VOIs were centred using the CT image. Low contrast between the plastic spheres in the NEMA body phantom and the surrounding media prevented a full size VOI from the SPECT measurement to be centred, which lead to the use of a smaller VOI, 70% of true volume size. This 70%-VOI size was used for evaluation and the results were used when comparing the PET to the SPECT images.
With the PET-camera system it is optional to choose a shorter acquisition time from a specific measurement. This was performed in order to find out if a shorter acquisition time than 30 min for SIRT-treated patients is possible, considering the low positron branch and also the low statistics. The patient can, of course, not spend too much time in the PET-camera. The first of the total four 30 min scans was reconstructed with shorter acquisition times, that is: 20, 10, 5, 2 and 1 minute. Even though 1 minute is less likely to give a good image the PET-cameras possible limitations could be interesting.

8.1 Quantification of ^{90}Yttrium

For this evaluation, a 9 mm in diameter larger VOI than the true spheres were applied both on the PET and SPECT measurements as used in “recovery coefficient ^{90}Y” above.
Results were analysed with different number of iterations. As previously stated; larger VOIs than the spheres is not a conventional method of quantifying activity concentration, but perhaps still applicable, since only a relative result is required in order to compare PET-camera with the SPECT-camera measurements.

9 Patient evaluation 1

Last fall a double post-SIRT measurement was performed. The patient received an administered activity of 1230 MBq ^{90}Y. The method for quantification was threshold based segmentation performed in AMIDE. The threshold for the PET-measurements was 100 kBq/ml and 50 kBq/voxel for the SPECT measurement, due to the double voxel size in the SPECT images. PET-images were reconstructed with 3 iterations and 12 subsets. Since the data had disappeared from the hard drive no additional reconstructions could be performed. SPECT images were reconstructed with 50 iterations and 12 subsets.

9.1 Patient evaluation 2

The patient for SIRT-treatment in May was administered 1030 MBq into the liver. The patient was measured both in the PET-camera and the SPECT-camera. Once again segmentation based threshold was the evaluation method used in AMIDE. A larger number of iterations could be performed since the measurement had not

been deleted from the hard drive as was the case with the first patient measured in the PET camera.

9.2 Patient evaluation 3

A third and also a fourth patient were SIRT-treated in June. The third patient received 790 MBq into the liver. Patient three was measured in both PET- and SPECT camera for comparison. Segmentation based threshold was used for the quantification evaluation. Patient four did not complete both measurements, thus no results are presented.

10 and 10.1
Simulated "liver" with ^{90}Yttrium

Due to gravity and segmentation problems with the SIR-spheres, a solution based on gelatin was used. This was mixed up in a theoretical "liver" volume of 1.5 litres. This "liver" was scanned both in the PET and the SPECT camera. ^{90}Y activity inserted in the "liver" volume was about 800 MBq.
Later on, small plastic vials with different amount of activity were inserted into this "liver" volume. The simulated "liver" was put into an empty phantom which was filled up with water. This water phantom was about 10.7 litres in total and elliptical to simulate a patient torso. PET and SPECT scans were performed in an upright position; otherwise the "liver" volume could move during scan. Figure 7 shows the finished phantom.

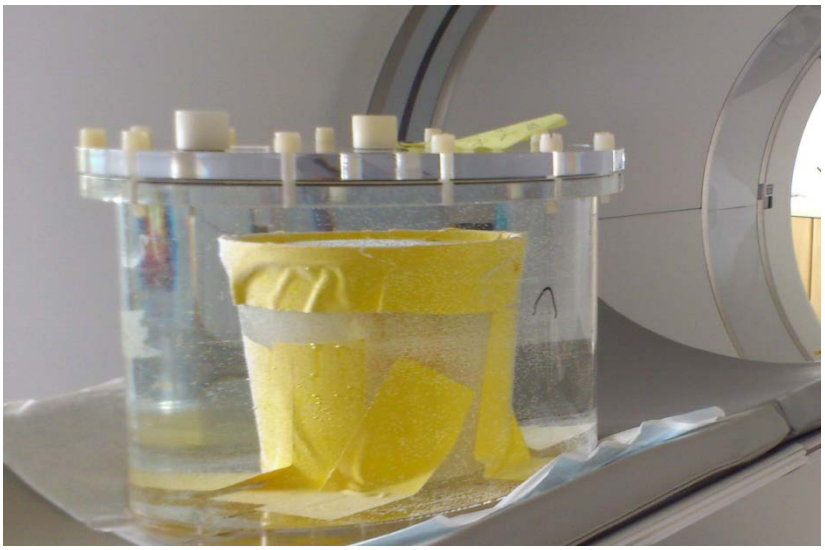

Figure 7. Simulated "liver" volume in water phantom before entering the PET-camera.

In total the activity was about 1000 MBq of ^{90}Y. However, this is a rather uncertain number due to some problems when creating the phantom. First the spoon which was used for stirring became contaminated and thus contained some unknown ^{90}Y activity. A rough and generous estimation is that the spoon contained 2% of the total activity.
The plastic vials were measured, but in a wrong geometry for the calibration

settings of the ion-chamber. A 20% error was set to this measurement. To these errors the ion-chamber calibration error is added, which is 5%. In total the error bars became 10%.
Much effort was given to analyse the results from the PET and SPECT measurements. Threshold based segmentation was applied in AMIDE. Corrections for the fact that the SPECT values are given in MBq/voxel and the PET values are given in Bq/ml had to be performed. The threshold for the SPECT-images then became 50 k Bq/voxel and for the PET-images it became 100 kBq/ml, since one SPECT voxel was about 0.5 ml.

When measuring the "liver" volume without surrounding water only one Bed-position was required to cover the volume. With the water phantom around, two Bed-positions were required. A longer acquisition measurement of 60 min per Bed-position with the PET-camera was also performed on this setup.

The SPECT measurements were performed with 60 angles each of 60 seconds acquisition time. For attenuation correction the CT-scan was used. SPECT images were reconstructed in **LundAdose** which uses the OSEM algorithm with 12 subsets and with an optional number of iterations.

10.3 Simulated "liver" with ^{90}Yttrium

Since a second opportunity appeared to create phantoms with ^{90}Y, because of leftovers from SIRT-patients, an easier and more accurate experimental strategy was invented.
The same "liver" volume as used in previous experiments was used. This time no hot vials were produced, and the aim was simply a homogenous activity distribution. Gelatin was used again, but the ^{90}Y activity was inserted earlier than previous experiment. The stirring spoon was replaced with a condom covered glass rod, to avoid contaminating the material. When the gelatin was stiff enough the protecting condom was detached from the glass rod. No spill from the measured ^{90}Y activity could be noticed. Inserted into the "liver" volume was 1550 MBq of ^{90}Y which was then placed at the bottom of the same water phantom as used previously (Figure 7). Measurements were performed both in the PET- and SPECT-camera.
To test the possible Bed-overlap issue, different settings with the overlap were performed. It consisted of one normal scan, one with the largest possible overlap and one with minimal possible overlap. Comparisons between these different measurements were analysed.

10.4 Bed overlap with simulated ^{90}Yttrium

Since the previous patient measurement showed a string of additional activity across the Bed-overlap this measurement was performed. In this experiment ^{18}F became a substitute because no ^{90}Y was available at SUS in Lund.

The “liver” volume was filled with about 200 MBq ^{18}F. Next day PET-measurements were performed. One respective two Bed positions were performed for the setup. ^{90}Y protocol was used for all measurements. The ^{18}F activity was multiplied with a factor of 30 220 in the calculations, to simulate the positron branch from ^{90}Y. Decay correction was performed as described in equation (8).

The ambition was to see different quantification results depending on how many Bed positions used in the measurements.

Results and discussion

4 Activity Quantification of ^{18}Fluorine

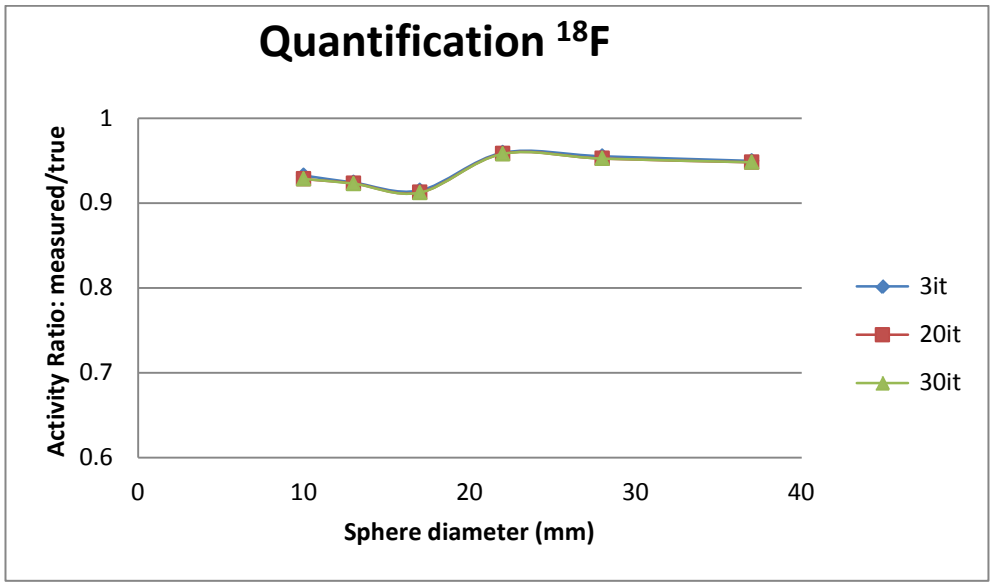

Figure 8. Total activity within a large VOI as a function of sphere size. Also is shown the different number of iterations.

Table 4. Relative background noise level with different number of iterations.

# Iterations	Relative background noise
3	100%
20	156%
30	158%

As can be seen from Figure 8 the PET-system recovers the theoretical activity within an accuracy of 94% in average. Since the defined VOIs are larger as compared to the actual volume of the sphere it is expected that almost all counts will be included within this VOI. A disadvantage of using large VOI is that counts from external activity, such as activity within the pipe, will be included in the activity calculation. Also minor deviations in sizes between the different spheres may be due to small water drips left in the spheres before the activity was injected. Furthermore, small air bubbles can influence the activity quantification. This would have a larger effect on the smaller spheres than the bigger spheres, relatively seen, this can also be suspected from the diagram.

There is no significant improvement when using an increased number of iterations. The background noise is affected though, as can be seen in Table 4 which is expected as the iterations increase.

4.1 and 4.2
Recovery Coefficients and different background ratios with ^{18}Fluorine

There is a significant difference between small and large spheres when comparing the activity concentration obtained from reconstructed images with the known objects activity concentration. This is generally termed the partial volume effect (PVE) [27, 28]. Since the spatial resolution for PET cameras is limited, due to the parameters discussed in the theory section, the result cannot be expected to be 100%.

A correction of the results is therefore necessary to compensate for the PVE effect. One approach of such correction is to apply the recovery coefficients (RC) which is an easy implementation. In clinical application this probably may not be accurate since some types of cancer tumours do not have spherical shapes. Nevertheless, the PVE is an important fact to keep in mind when the aim is to quantify SUV values within small tumours. As a rule of thumb the approximate object size required for an accurate reconstruction of the activity concentration is approximately 2-3 times FWHM, without loss of linearity, which seems to match the results [29].

From Figure 9 and 10, it is shown that there is a difference in the results when increasing the number of iterations. It seems like a better result is reached with an increased number of iterations. Only a small change in the result is noted when comparing 20 and 30 iterations. An increased number of iterations for the purpose of activity quantifying could be applied post-acquisition and thus would not affect the patient flow through the clinic. The result implies that for the best separation of different levels of activity, at least 20 iterations are required. This is useful if a calculation of the absorbed dose would be performed. The result when not using the TOF seems to be accurate, as can be seen in Figure 11. However, this graph is maybe somewhat misleading since it only shows the activity ratio, which seems good for non-TOF. The results are best presented in Figure 10.
The sphere- to- background ratio also affects the result due to the “spill-in” and “spill-out” of counts which has a more pronounced effect when the activity quotient is larger. A background activity closer to the spheres´ activity makes the spheres´ recovery look better due to the fact that the spill-in exceeds the spill-out effect.

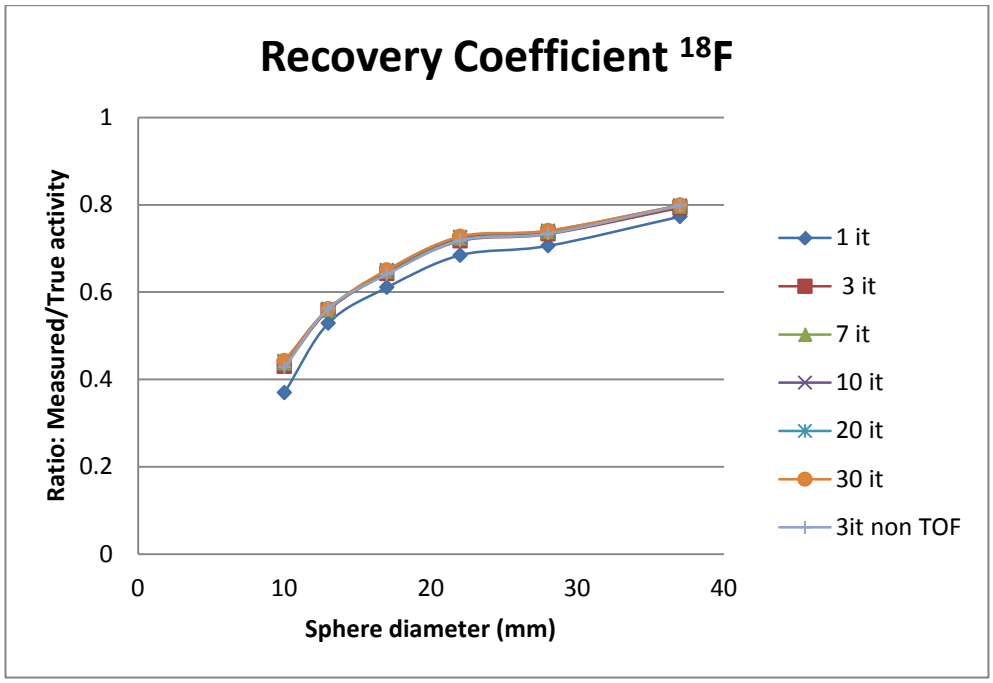

Figure 9. Recovery coefficient for the measurements with the NEMA body phantom with sphere sized VOIs. The graph also shows the different number of iterations as well as without TOF.

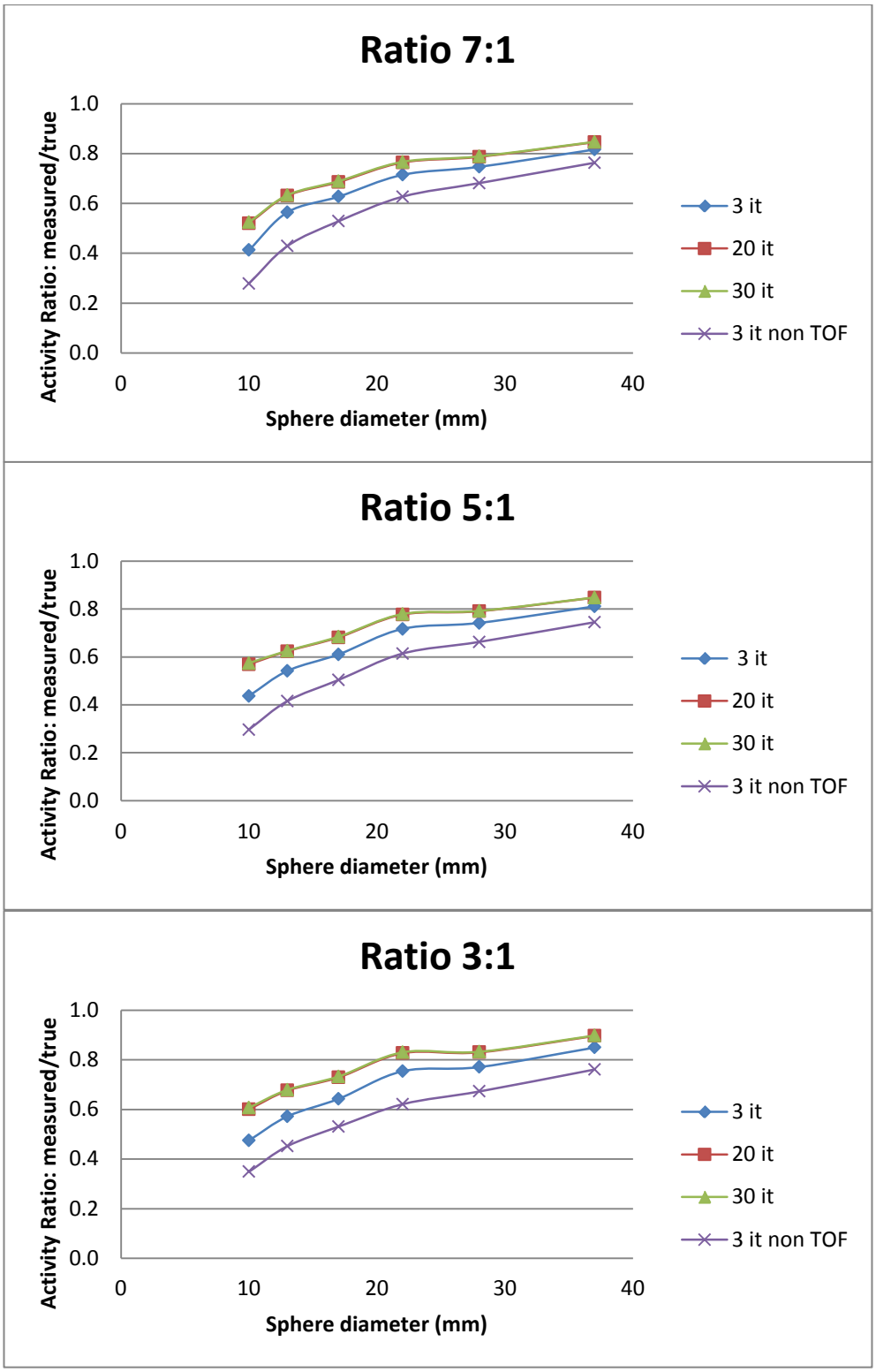

Figure 10. The activity ratios as a function of sphere diameter and with different number of iterations. Results also includes without TOF.

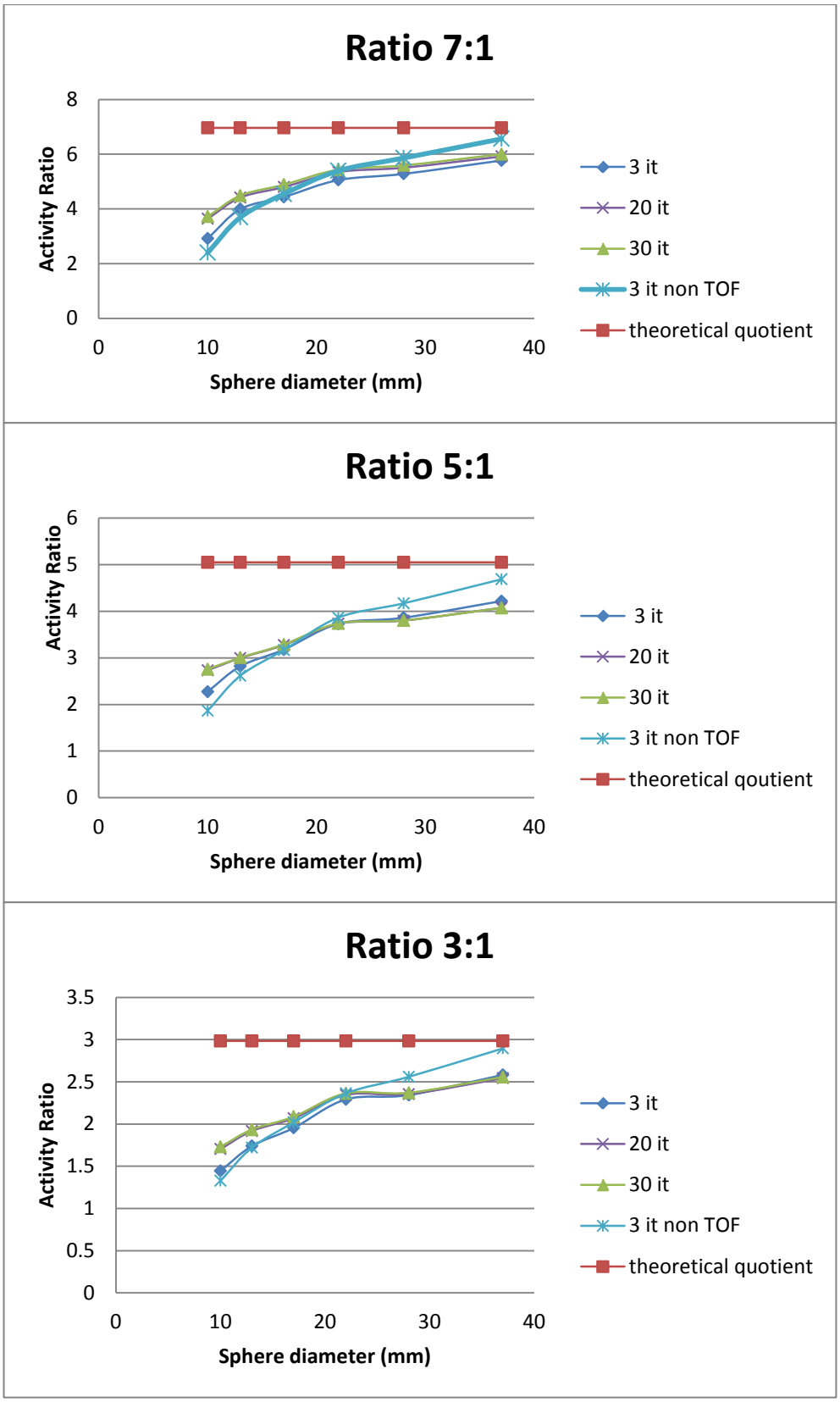

Figure 11. Activity ratios from the measurements performed, shown with different number of iterations and without TOF.

Regarding the Recovery comparison plot, Figure 12, there are significant differences worth noting. The 70% VOI has the best match out of these since a smaller VOI excludes many of the voxels affected by the PVE, which is the spill-out. An even better result is reached with the smaller 12.5%-VOI. For this VOI-size the only large deviation is the smallest sphere (10 mm in diameter). Maximum values do not match the line profiles in Figure 13. This is probably because of that the line profile drawn did not pass through the maximum pixel value.

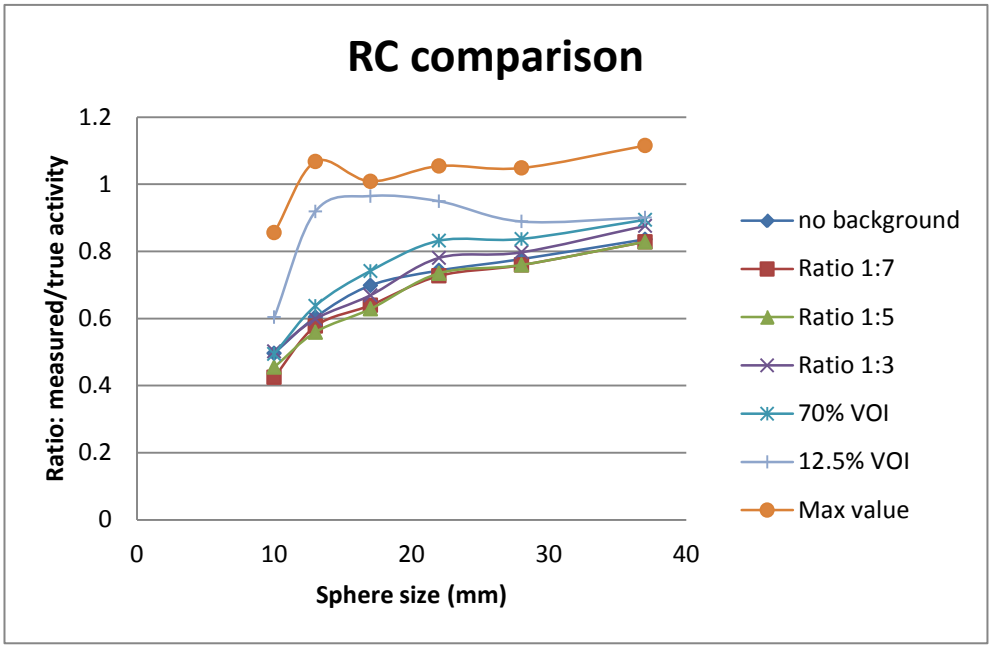

Figure 12. Recovery coefficient comparison for the standard protocol, that is with 12 subsets and 3 iterations. Here presented with and without background activity complemented with max value, 70% and, 12.5% VOI without background activity.

The line profiles plotted in Figure 13 shows that the maximum value is rather constant for spheres larger than approximately 2.4 times FWHM. The two smallest spheres do not have as large maximum values as the others due to the PVE, as illustrated by Soret et. al in the figure below, figure 14 [27].

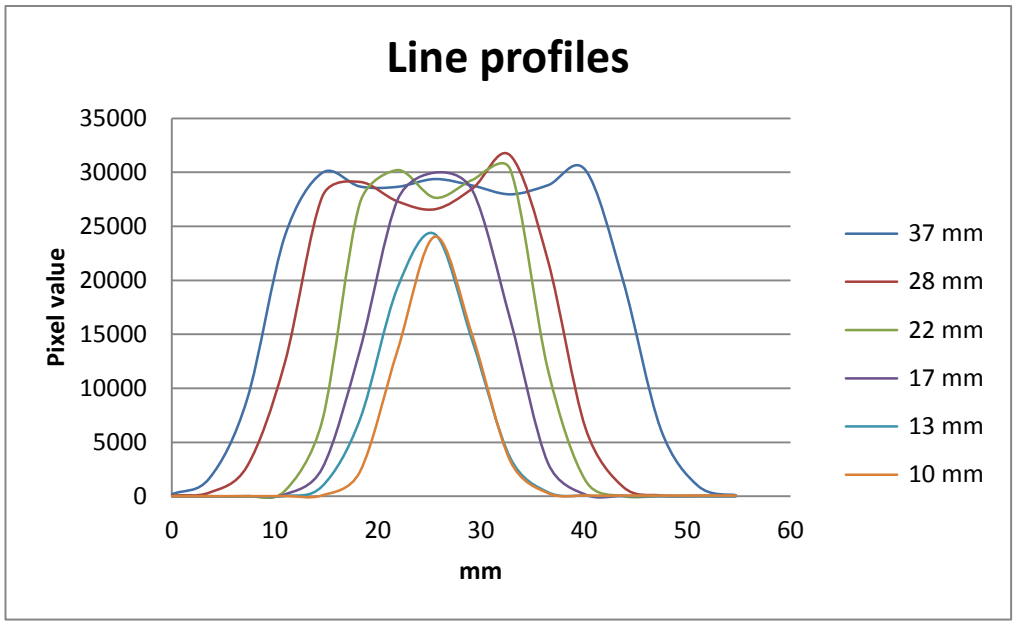

Figure 13. Line profiles with intensity as a function of distance and with different sphere sizes.

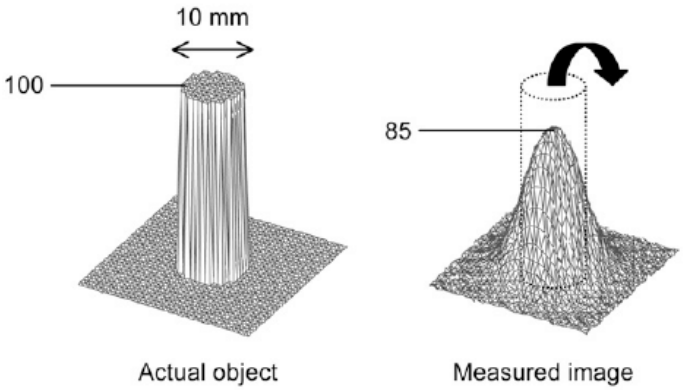

Figure 14. The partial volume effect illustrated [27].

5 Spatial resolution

Table 5. Results from the spatial resolution measurement with ^{18}F and ^{90}Y.

^{18}F 192x192 matrix	Thick line	Thin line
FWHM	8.1 mm	6.5 mm
^{18}F 256x256 matrix		
FWHM	7.3 mm	6.2 mm
^{90}Y 192x192 matrix		
FWHM	7.1 mm	5.9 mm
^{90}Y 256x256 matrix		
FWHM	6.7 mm	7.0 mm

The spatial resolution results, shown in table 5 were not as accurate as expected. This might be due to the fact that the NEMA protocol was not used. The numerical values would probably be in better agreement if a correct measurement, according to the NEMA protocol, is performed. Measurement according to the NEMA standard was conducted during the acceptance tests of the PET system and showed satisfactory results. The differences between the NEMA standard test and the measurement performed in this experiment is that filtered back projection is the standard reconstruction method regarding the NEMA protocol and OSEM is the reconstruction method used in this experiment. Also there is a difference in post-filtration of the image. In the NEMA standard there is no post-filtration performed as there is on a clinical PET measurement [30].
An additional reason for the numerical value being larger than expected may be the possibility for the positrons to interact in the plastic compartments above and beneath the line source. This can produce a wider FWHM compared to a small point source surrounded with air, as in a NEMA standard measurement. Also noteworthy is that a thinner line source results in a smaller FWHM for ^{18}F but not for the larger matrix size and ^{90}Y. Since the values are small and the line profile performed in AMIDE is arbitrarily set, the result may vary because of this.

According to the manufacturers data, the spatial resolution should be 4.9 mm at a distance of 1 cm from the centre [16]. If a linear relationship in the transaxial direction could be assumed for the FWHM this would give a value of 5.2 mm for the FWHM at a distance of 5 cm off-axis.
When using a larger image matrix size the value for the FWHM was improved for ^{18}F but degraded for ^{90}Y. One possible explanation is that a lower statistical readout per voxel gives a wider Gaussian for the 256x256 matrix as compared to the 192x192 matrix.

6 Beta spectrum from ^{32}Phosporus

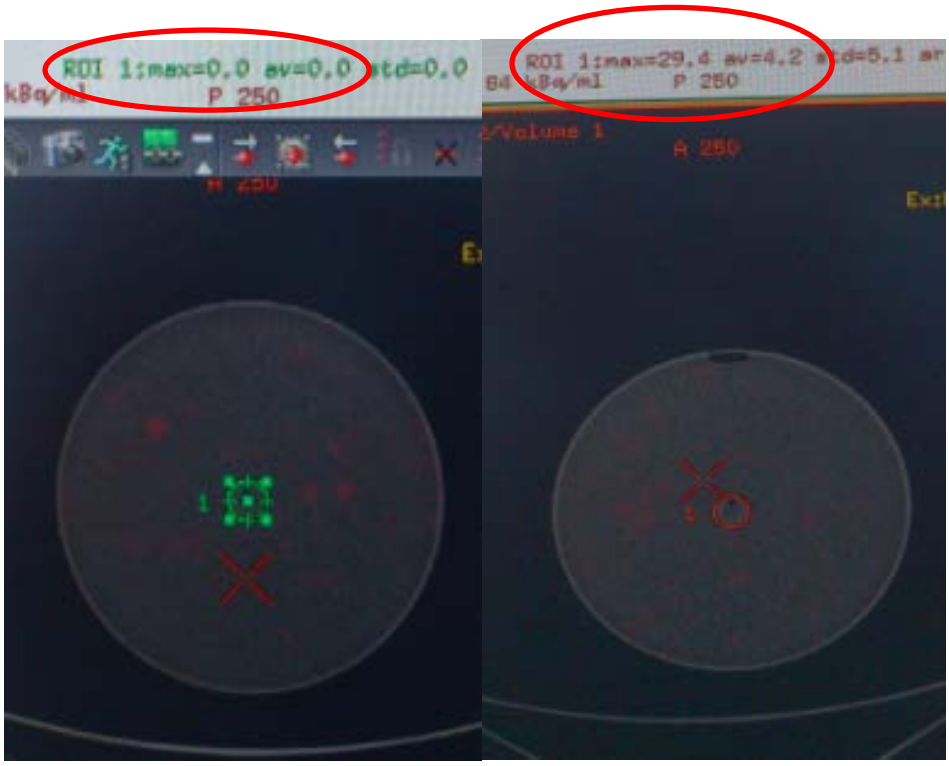

Figure 15. To the left a measurement with a sphere containing ^{32}P and using the ^{18}F acquisition protocol is shown. To the right the same phantom setup but now acquired with the ^{90}Y protocol is shown. Images were evaluated at the workstation connected to the PET system.

As can be seen in Figure 15, there is a significant difference regarding the measured activity. With the ^{90}Y protocol there is an activity in the image, in contrast to the F-18 protocol where no activity is measured.
This result seems to be dependent of which protocol used. Since only about 32 ppm positrons can be expected from ^{90}Y, as compared to 96.7% for ^{18}F there is a large difference in how the overall counts are being scaled dependent on the protocol being used. The hotspots in the PET image can probably be referred to background noise which is multiplied with a factor k.

$$k = \frac{0{,}967}{32*10\text{^}-6} \approx 30\,220 \qquad (9)$$

That gives rise to the apparent 'activity' in the image. One potential source of additional counts appearing in a voxel may be the low activity in the LYSO crystals itself. According to Bettinardi et al [22] this natural activity in the crystal material would contribute the count rate with about 1 cps, thus this should not produce a significant contribution. However, when scaling with the factor k of about 30 000 this becomes somewhat greater and perhaps significant. Another possible explanation to these hotspots is the multiplicative factor combined with an incorrectly calibrated detector-pair. An inaccurate normalization of the detector-pairs can lead to an increased image noise [19].

The PET camera does not mistakenly refer any bremsstrahlung photons from the ^{32}P sphere to be a true coincidence, and the branch of positrons from ^{32}P is most likely too low to be detectable, at least with this low activity. If a larger activity would be used, maybe it would be possible to get an image as well. The activity required would be very large though.

6.1 Background level

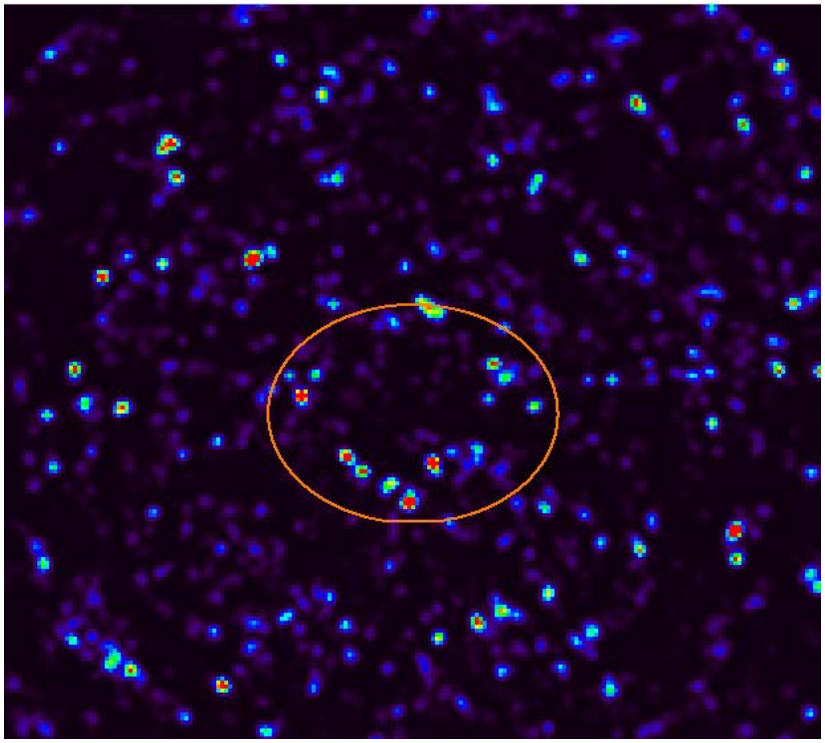

Figure 16. Image showing the blank scan measurement and the VOI in one plane.

Table 6. Background level measurement.

Protocol	Mean value (Bq/ml)	Measured Quotient	Theoretical Quotient
^{18}F	0.05		
^{90}Y	1563	30842	30220

As seen in Table 6 there is a clear relationship between the background noise level and the theoretical assumption of a matrix multiplication. As assumed the difference is a factor of about 30 000.

If the background value is multiplied with the volume the total activity is determined. This shows that approximately 1 MBq exist in the image from the ^{90}Y protocol. Even though there is zero activity in the ^{18}F measurement.
A possible source for this background level is the low content of ^{176}Lutetium in the LYSO crystals within the PET´s detector rings. These unwanted extra counts would need to be corrected for, in order to make an accurate activity quantification, as suggested by Gates et al [13].

7 ^{90}Yttrium simulation

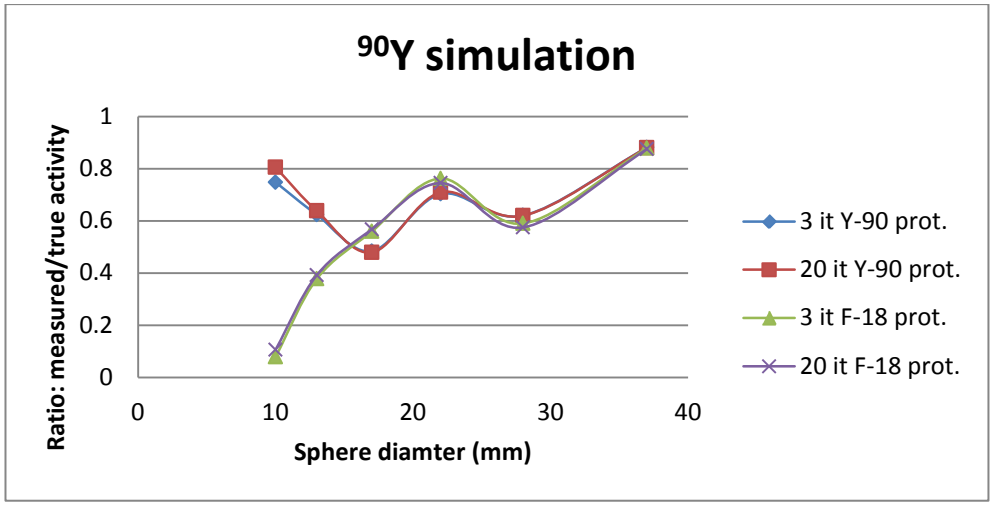

Figure 17. Graph showing the activity ratio, and comparing the ^{90}Y protocol with the ^{18}F protocol.

A large difference between the different protocols used is seen in Figure 17 for the smaller spheres. This is most likely not because of the more accurate measurement with the ^{90}Y protocol but because of the influence of background noise. The absolute values are better for the larger spheres in this measurement than for the RC curve. This is most likely due to background noise as well. A small number of counts are more affected by a background noise than a large number of counts, relatively seen.

8 Recovery coefficient ^{90}Yttrium

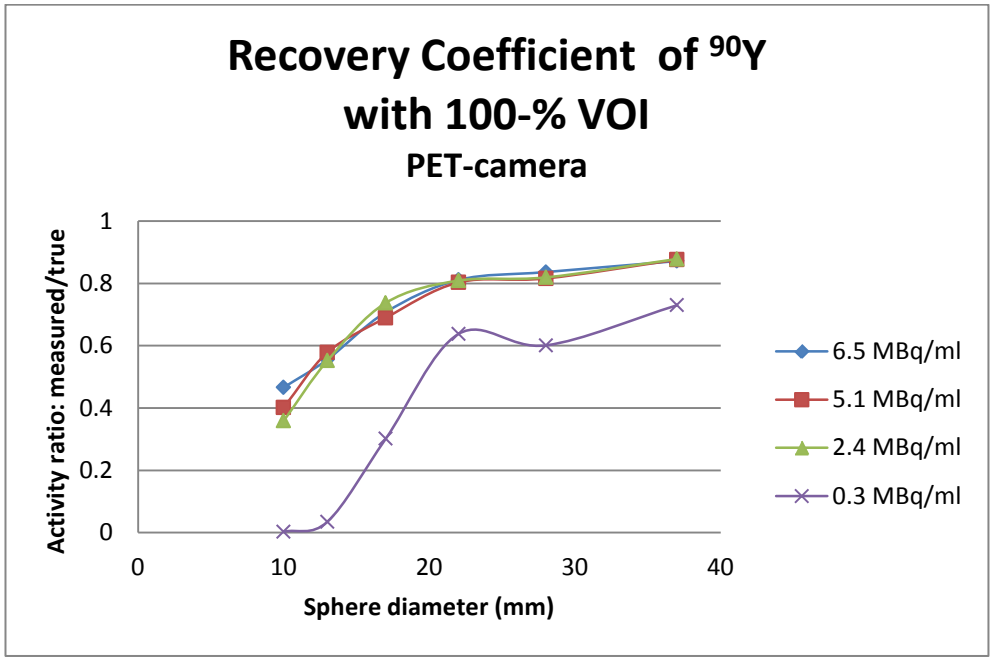

Figure 18. Recovery coefficient measured with Y-90 in the PET-camera. The curves present different activity concentrations with the RC-curve as a function of sphere diameter. Sphere sized VOI was used for all these measurements.

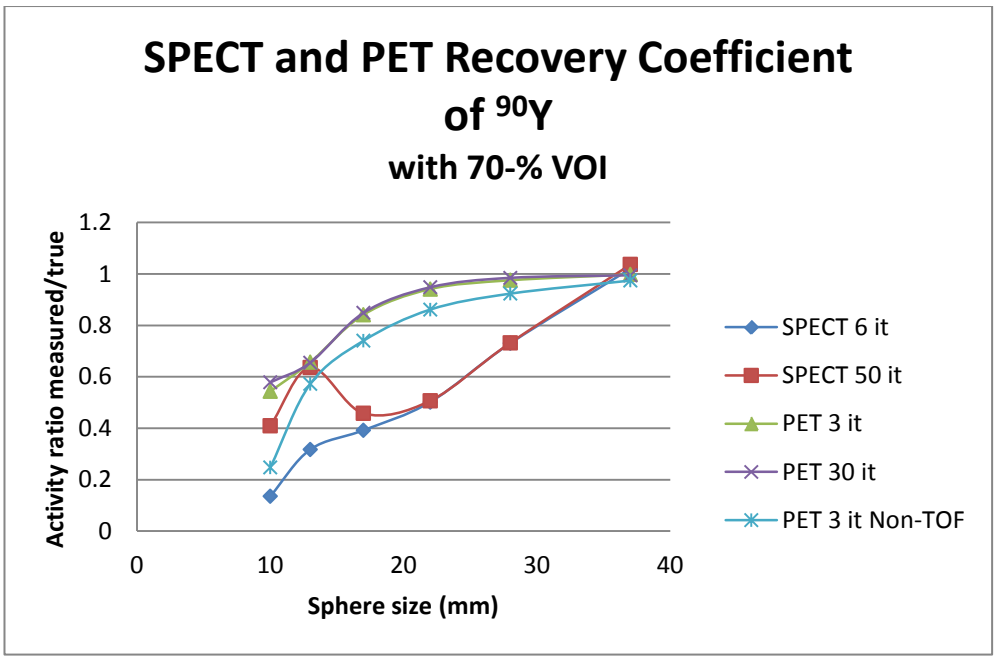

Figure 19. Comparison of RC curve between PET and SPECT measurement.
Also included is the non-TOF reconstruction.

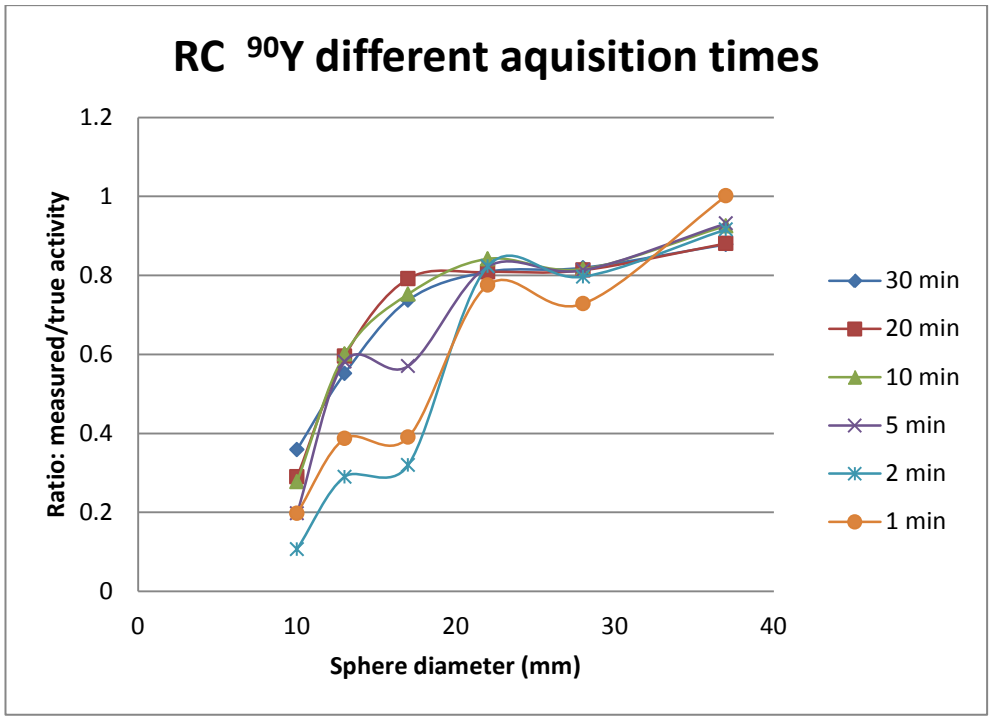

Figure 20. Recovery curves with different acquisition times.

The recovery curve for ^{90}Y, in Figure 18, is very similar to the RC-curve performed with ^{18}F, Figure 9. The relative value is higher though, which is most pronounced for the larger spheres. This might be because of more background noise in the image as discussed before.
Interesting is that with the lowest activity concentration the curve becomes very deviant. It seems as if there exists a least required activity concentration necessary for the PET-camera. Also it seems like a nonlinear relationship with respect to spheres size is apparent. The smaller spheres´ recovery is much worse than the larger ones. Noteworthy is that there is a large eight time difference between the two lowest activity concentrations. Values in between is expected.

Regarding the comparison between the PET and SPECT camera measurements in Figure 19, it seems like the PET-camera system has a more consistent behaviour. Except for the non-TOF reconstruction results, which are worse than with TOF. No point of the curve is better with the SPECT-system than the PET-system. The only spheres that come somewhat near the PET result are the largest and the second smallest. Unfortunately for the SPECT-system this behaviour does not seem linear with sphere size.
When comparing different acquisition times as in Figure 20, there is a large difference between the curves. Even though an acquisition time of 1 or 2 minutes is not of relevance, it is of interest to see the behaviour of the quantification results with short acquisition times. At least a 10 minute scan seems necessary for a stable result.

8.1 Quantification ^{90}Yttrium

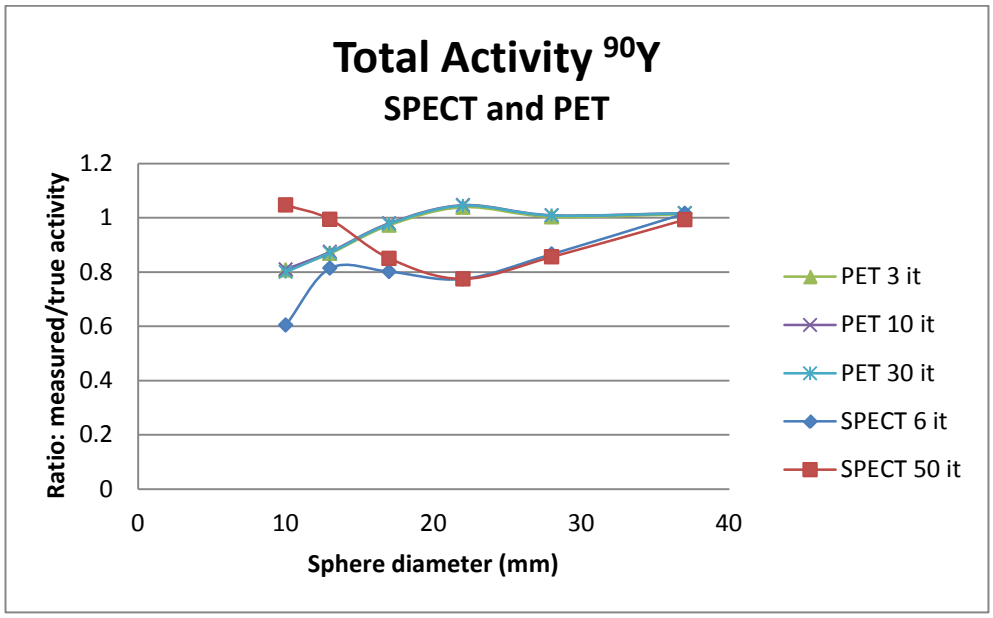

Figure 21. Comparison of the total activity measurement with PET and SPECT camera. A VOI larger than the actual sphere are applied and evaluated.

Figure 21 shows the result from the SPECT and PET measurement.
It can be seen that there once again is a difference between 6 and 50 iterations for the SPECT measurements. Fifty iterations seem to give a better result than 6 iterations. An unexplained decrease is seen between the 13 and 37 mm sphere. A possible reason would be inhomogeneous activity concentration. However, the PET curves are not showing any sign of an inhomogeneous activity concentration. Perhaps something in the reconstruction algorithm performed at the SPECT images could be the explanation.

The PET curves do not show any improvement when performing more iterations. To keep in mind is that these measurements are performed with an activity concentration of about 6.5 MBq/ml, which implies good statistics.

9 Patient evaluation 1

Table 7. Results from patient 1.

Patient 1	Measured activity (MBq)	True activity (MBq)	Deviation
PET 20 min per BED (3 it)	1233	1018±72	+19%
SPECT 30 min (50 it)	1009	1007±71	+0.1%

The results provided in Table 7, show that the PET-camera overestimate the activity with about 20% as compared to the results obtained with SPECT which is good agreement for the activity quantification.

The error in the measurement of the true activity is estimated to 7%, where 5% relates to uncertainty in the ion-chamber calibration and the additional 2% from the geometric uncertainties when measuring the catheters, needles and containers after the SIRT-treatment.

The SPECT camera is well within these error bars but the PET-camera overestimates the total activity with 19% and thus is beyond these error bars. Even though these values could be refined with other thresholds (larger) this was not performed. The reason is because it is desired to cover up the whole liver with the segmentation. With a larger segmentation to many voxels which contains activity is excluded and thus gives a closer match to the total activity aimed for, since the total activity is overestimated. This would of course not show the accurate result. Perhaps a larger threshold could be used if a least activity is decided for absorbed dose calculation.

The overestimation for the PET-system is interesting. One possible reason, again, is the additional counts from the LYSO-crystals, which has not been corrected for in the activity quantification. This since no good method could be figured out to apply on such subtraction. However, such a subtraction must be performed before computer system creates the tomographic images. Since the PET -camera is considered a black box when it comes to performing changes on calculation steps this would not be possible within this project.

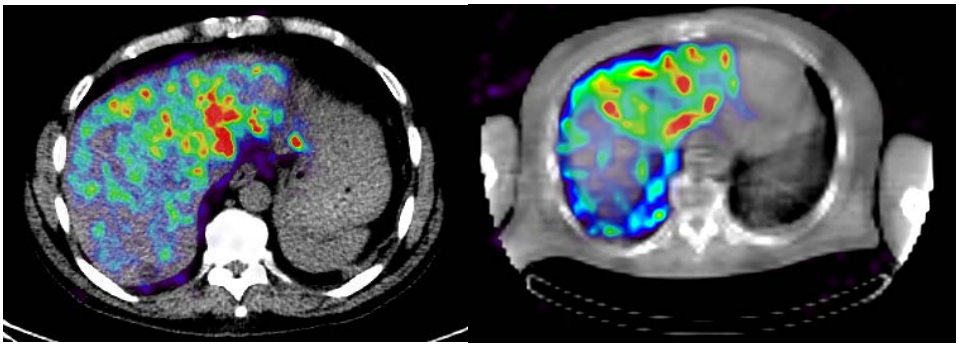

Figure 22. To the left the PET-image from patient evaluation 1. To the right the SPECT-image from the same patient.

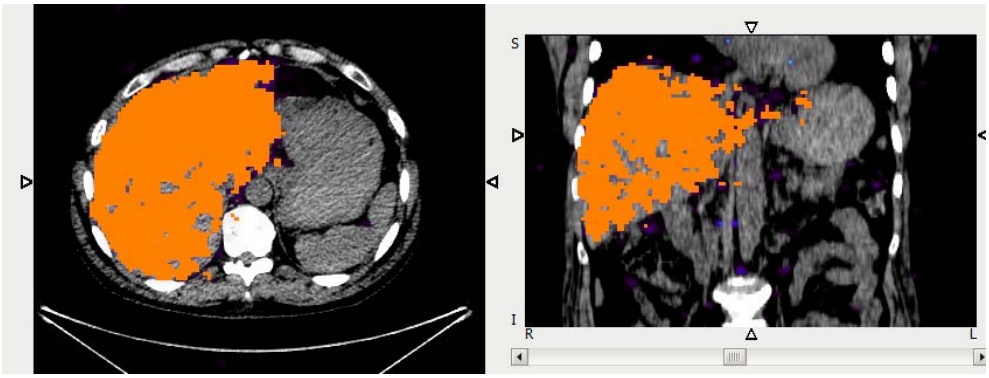

Figure 23.PET-images from patient 1 showing the segmentation applied in coronal and transversal direction.

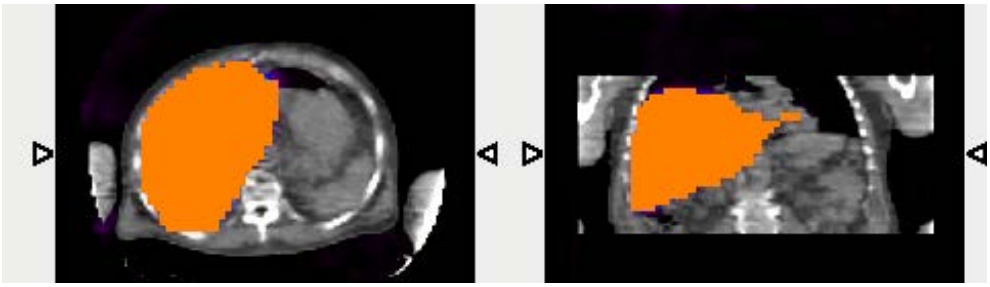

Figure 24. SPECT-images from patient 1 showing the segmentation applied in coronal and transversal direction.

9.1 Patient evaluation 2

Table 8. Results from patient evaluation 2.

Patient 2	Measured activity (MBq)	True activity (MBq)	Deviation
PET 20 min per Bed (3 it)	964	821±58	+19.4%
PET 20 min per Bed (20 it)	1013	821±58	+23.4%
SPECT 30 min (50 it)	725	812±57	-10.7%

Also in this evaluation the activity concentration from the noisy PET-image shows an overestimation of total activity as presented in Table 8. The result is about the same as the first patient evaluation. An underestimation from the SPECT-measurement is also seen for this patient. A better result could also be obtained if a smaller threshold were applied. But if a smaller value of the threshold were applied in the SPECT-images a smaller threshold would thus be necessary in the PET-images in order to keep the ratio about 2 because of the ml per voxel relationship. This would give a larger overestimation in the PET-images and also add more background noise in the total activity quantification. A perfect threshold for segmentation purposes is difficult to determine.

Surprisingly when looking at the maximum intensity projection (MIP) -image at the PET workstation a possible Bed-overlap problem is apparent. This is visualized in Figure 25. From this Figure 25 it seems like the field of view overlap causes extra counts in the image. A possible explanation for this is the nonlinear sensitivity over the axial FOV. This is corrected for with a matrix to give an equal sensitivity along the FOV. This in combination with additional counts from the LYSO crystal elements could potentially increase the quantification result.

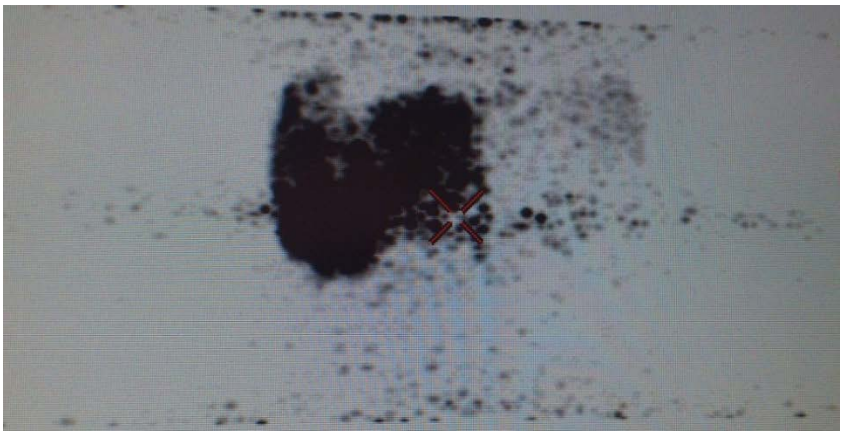

Figure 25. Possible Bed overlap problem shown. Maximum intensity projection (MIP) image from the PET workstation.

Image 26 and 27 compares 3 and 20 iterations, and shows that the hotspots seems more smeared out in the 3 iteration image. With 20 iterations the hotspots has a more homogenous distribution than with 3 iterations. Though, the voxels, and hence the absorbed dose, will be more affected by 20 iterations since the hotspots intensity is more pronounced. Perhaps a smoother distribution of the background noise is preferred if it cannot be subtracted. In addition the quantitative result does not become better with 20 iterations, but instead worsened by 4%. One should keep in mind that this is partly due to the threshold based segmentation evaluation method, which seems to add some of the hotspots surrounding the liver. Even though the 20 iteration image seems to have a more accurate activity distribution, there is a significant contribution to the total quantitative result from the hotspots surrounding the liver. Some of them could perhaps be accounted for because of respiratory motions during acquisition but some of them are most likely not supposed to contribute to the total activity. A more precise segmentation method is to prefer.

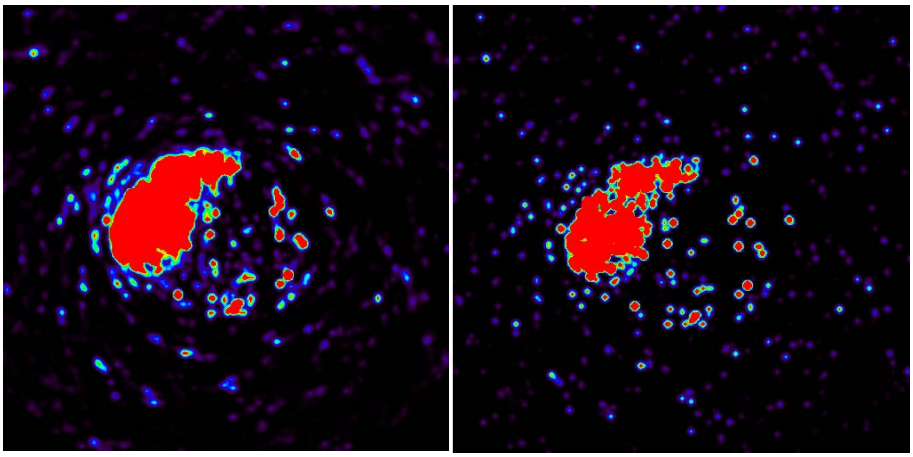

Figure 26. Three iterations PET-image of patient 2 to the left and 20 iterations to the right.

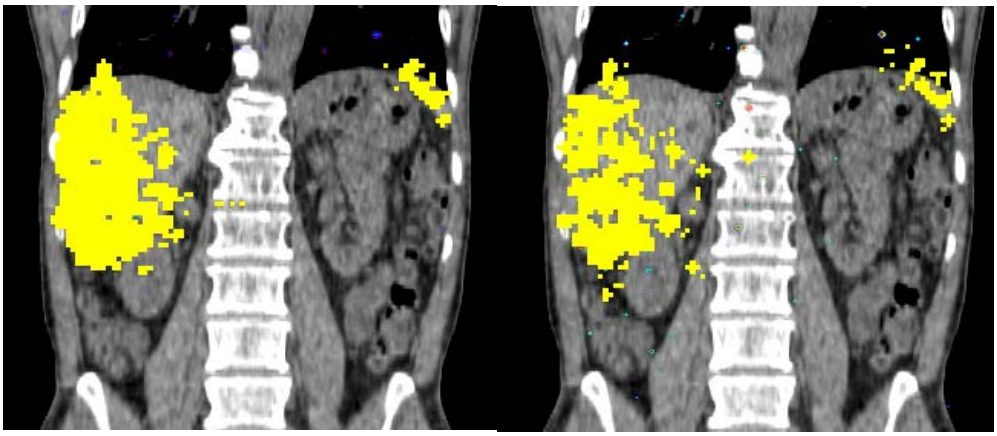

Figure 27. Images from AMIDE shows the threshold based segmentation VOIs applied on PET-images from patient 2. Three iterations to the right and 20 iterations to the left.

10 Simulated "liver" with ^{90}Yttrium

The results from this measurement were somewhat surprising, as presented in table 9. The SPECT camera has a minor deviation of about 2% whereas PET-camera underestimates the total activity with 18%. A low activity concentration is underestimated with the PET-camera as seen in Figure 18. This might affect the total quantification. Although the activity concentration in the "liver" volume would be at least:

$$\frac{800\ MBq}{1300\ ml} \approx 0.6\ MBq/ml \qquad (10)$$

The volume 1300 ml comes from the fact that it is impossible to fill the "liver" volume with gelatin, since a stirring was necessary and thus could lead to unwanted spill. Ultra sound gel was put on top of the "liver" volume to fill up the volume, after the vials were inserted.
The gelatine mixture with SIR-spheres did not become very homogenously distributed as seen in figure 29. This is probably because of the gelatin had becoming too stiff before the ^{90}Y microspheres were inserted.

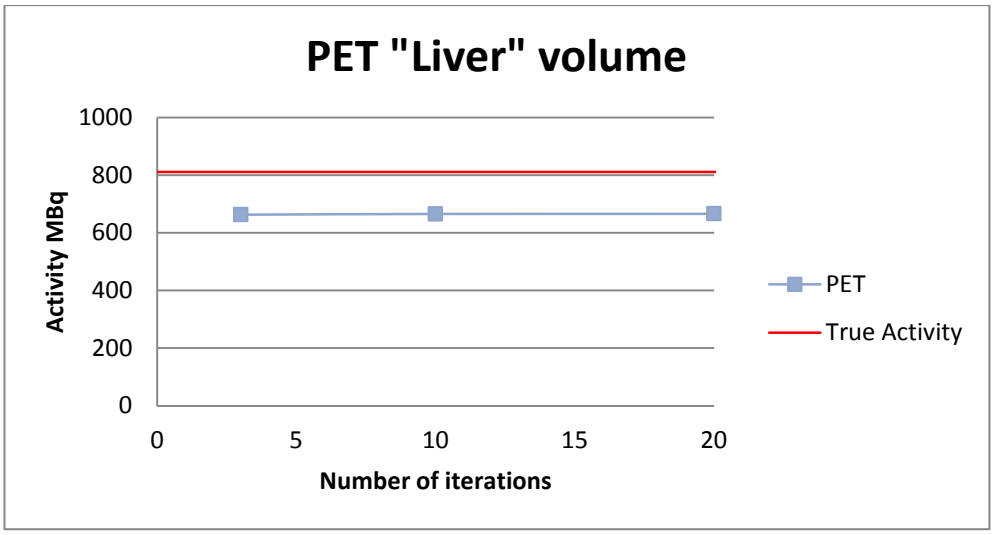

Figure 28. PET-quantification results from the “liver” volume alone. Total activity as a function of iterations is shown.

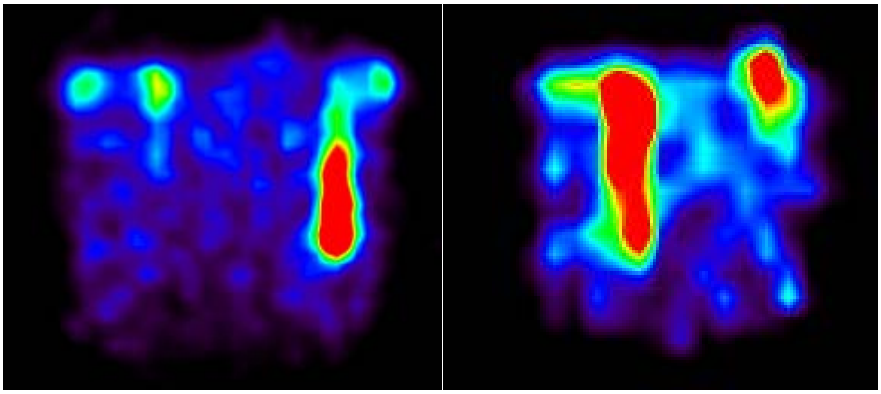

Figure 29. PET-image to the left showing the activity distribution in the “liver” volume, a similar image but with the SPECT-camera is shown to the right. The images do not show the same slice.

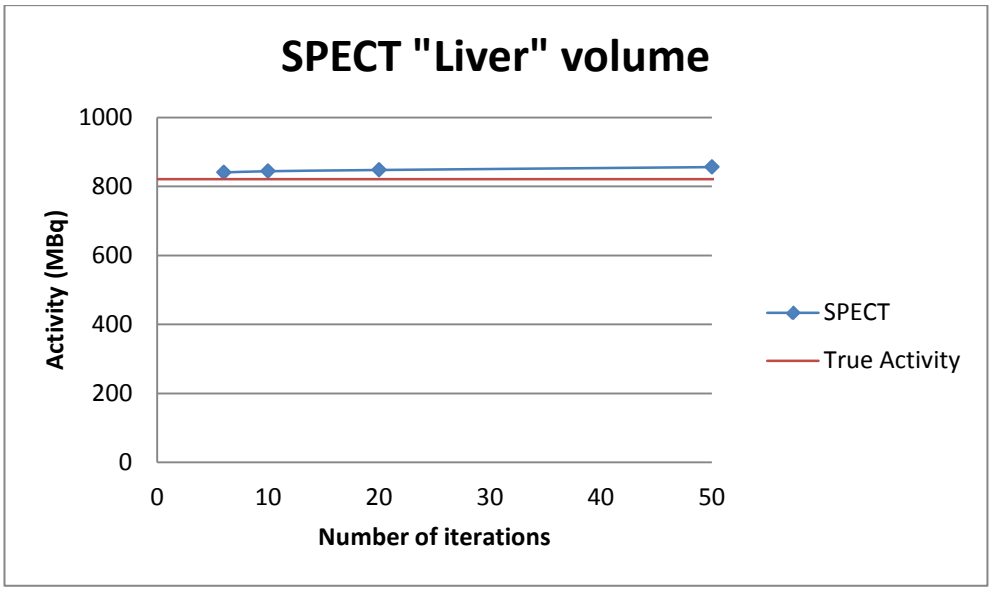

Figure 30. SPECT-quantification results from the "liver" volume alone. Total activity as a function of iterations is shown.

Table 9. The absolute values from the measurement with the "liver" volume. The PET value is from 3 iterations and the SPECT value is from 6 iterations.

"Liver" volume	Measured activity (MBq)	True activity (MBq)	Deviation
PET	663	811±57	-18.3%
SPECT	841	821±58	+2.4%

10.1 Simulated "liver" with ^{90}Yttrium

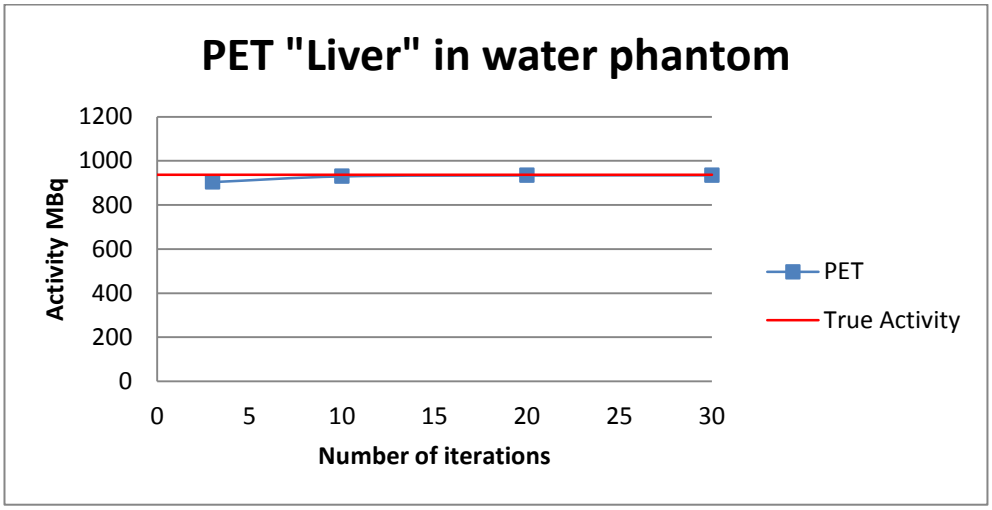

Figure 31. PET-quantification results with the "liver" volume in the water phantom.

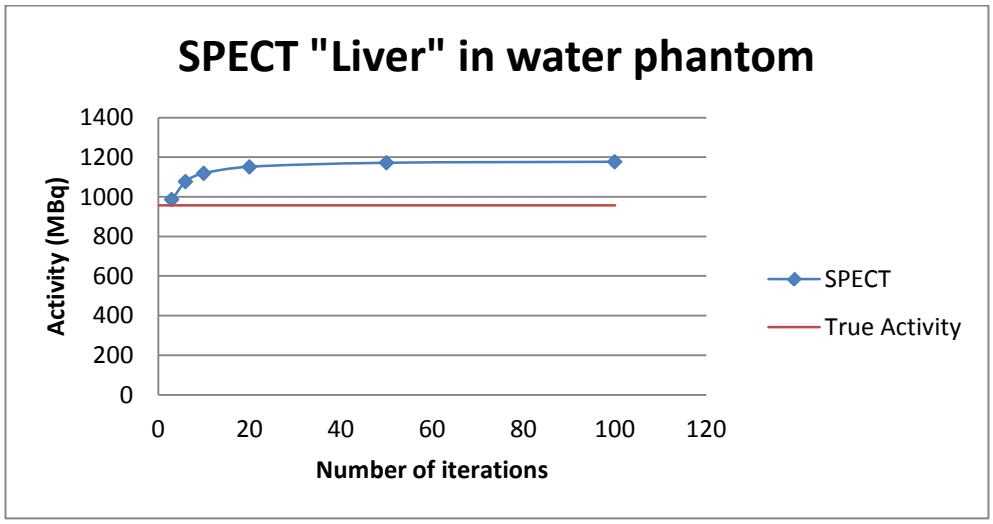

Figure 32. SPECT-quantification results with the "liver" volume in the water phantom.

Table 10. Results from the "liver" volume in water phantom measurement.

"Liver" volume in water phantom	Measured activity (MBq)	True activity (MBq)	Deviation
PET 30 min	1025	993±70	+3.2%
PET 60 min	903	966±68	-6.5%
SPECT 30 min	1134	983±69	+15.4%

The PET-camera shows a deviation of about 3% when quantifying the ^{90}Y content, as seen in Table 10. The SPECT-camera shows an overestimation of about 15%. One possible explanation to this is that the vials inserted in the "liver" volume contain more activity than expected. About 20% increase for both measurements indicates this.

The scan with 60 minutes per Bed -position shows a deviation from the 30 minutes scan of 6.5 %. A longer acquisition time should give better statistics and thus improve the quantitative result. This was not the case this time, even though the 10% error estimation is fulfilled. Thoughts of why the quantification result decreases with better statistics were awoken. A possible explanation is that the longer acquisition scan is the most accurate and that the small amount of overestimation is reduced with better statistics.

The only thing certain is that the PET and the SPECT camera show different results when quantifying ^{90}Y.

10.4 Bed overlap with simulated ^{90}Yttrium

Table 11. Different number of Bed positions with ^{90}Y simulation in the "liver" volume.

PET 20 min per Bed	Measured	Theoretical*	
# Beds	activity (MBq)	activity (MBq)	Deviation
1	2128	2201	-3.3%
2	1782	1844	-3.4%
1	847	876	-3.3%
2	715	748	-4.4%
1	494	502	-1.7%
2	409	426	-4.0%

*^{18}F converted to ^{90}Y activity

The results in Table 11 show no overestimation in activity for the measurements. Interesting is that the quantitative results are very close to the true activity. A source of error in this measurement is the fact that the water phantom surrounding the "liver" volume was not used; hence errors from the attenuation map could not be investigated. Measuring with the surrounding water phantom would also lead to a lower count rate than the one in this measurement. The initial count rate was 2.2 kcps and decreasing to 1.2 kcps for the last measurement.
If there is a contribution from a Bed-overlap as seen in image 25, the additional activity is most likely low.
The results also lead to thoughts of a large underestimation of the true activity in Table 9. If this is the case then the trend of an overestimation with the PET-camera and an underestimation with the SPECT-camera is almost verified. In contrast to this is the results seen in Table 10. Perhaps the first two measurement preparations with ^{90}Y cannot be taken too seriously since knowledge about the absolute ^{90}Y activity into the "liver" volume is unknown.

9.2[5] Patient evaluation 3

PET results in table 12 show again an overestimation of about 20%. The SPECT result on the other hand once shows an underestimation of about 15 percent. Since a smaller amount of ^{90}Y activity is expected in this patient's liver than previous patient´s, a quick thought of activity dependence for the SPECT-system is

[5] The results from this measurement were generated in this order, which is why it may seem strange to find "9.2" in the middle of the results from "10".

suspected. This since the expected activity has decreased with upcoming patients, and also the fact that the activity quantification has become more underestimated.

Table 12. Comparison of measured and true activity obtained for patient 3.

Patient 3	Measured activity (MBq)	True activity (MBq)	Deviation
PET 20 min per Bed (3 it)	761	632	+20.5%
SPECT 30 min (50 it)	529	625	-15.4%

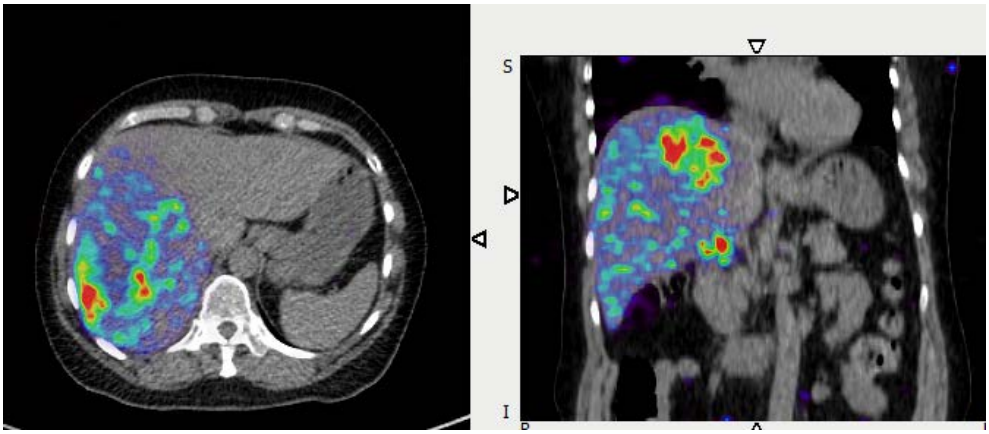

Figure 33. ^{90}Y distribution from PET-measurement in patient 3.

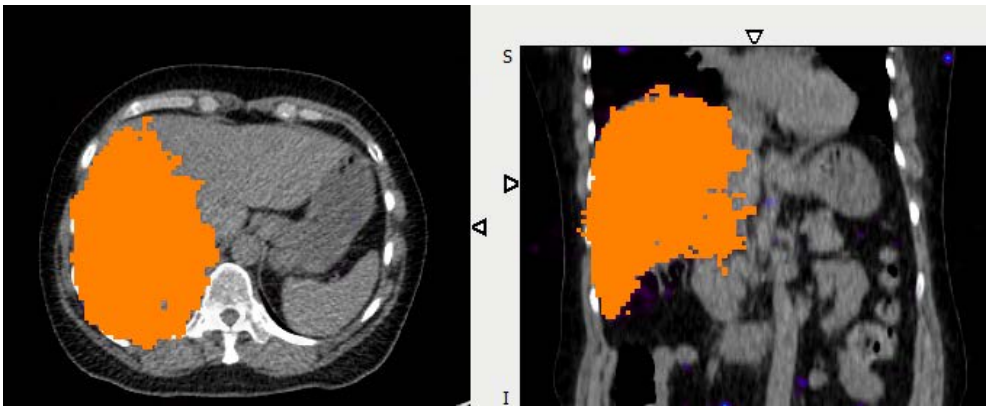

Figure 34. PET-measurement in patient 3 with the threshold based segmentation applied.

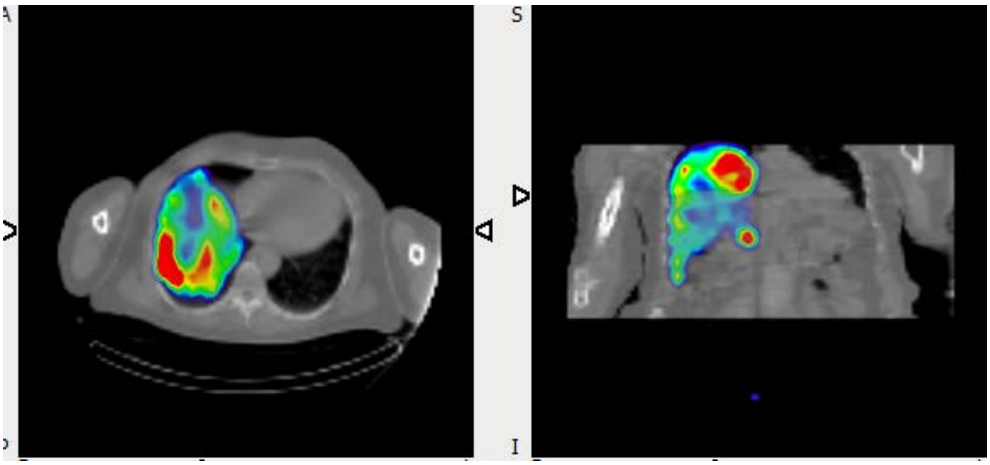

Figure 35. SPECT-measurement from patient 3 showing the ^{90}Y distribution.

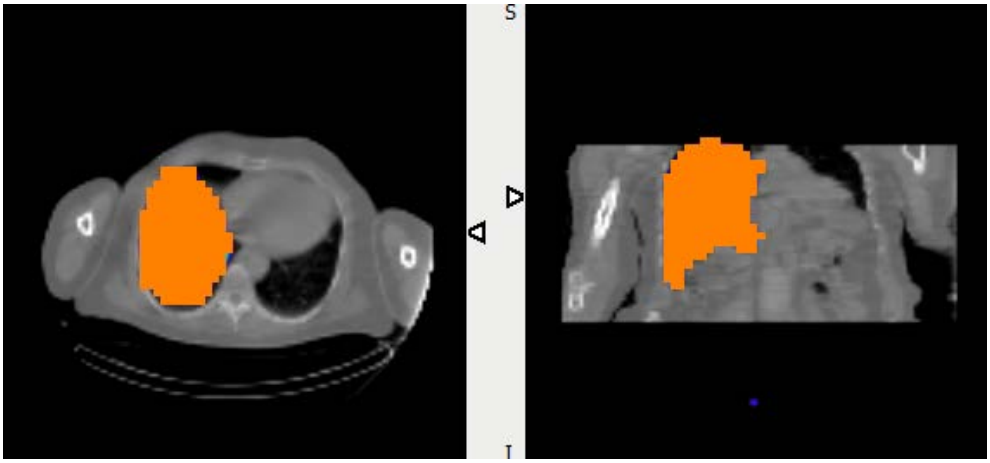

Figure 36.SPECT-measurement on patient 3 with the threshold based segmentation applied.

10.3 Simulated "liver" with ^{90}Yttrium

The results in Table 13 show a better quantification result for the PET-camera system than the SPECT camera system in table 14. The Bed overlap seems like a smaller problem from the PET-measurements.
A 5% difference between the smallest overlap and the normal overlap shows that there is a significant impact from the sensitivity differences in the transaxial direction. The "normal" overlap thus seems optimized since no larger difference is obvious when comparing with the largest possible overlap. A difference of 0.1% can be ignored.
A measurement in contrast to previous thoughts is the fact that one single Bed position does not overcome the results from two Bed positions. In fact the results show that the quantification results are about 6% better than with one Bed position.

Table 13. Results from the measurements of the activity in the "liver" volume inserted in the water phantom. Different Bed overlap possibilities were here compared.

PET measurement		Segmentation threshold = 100 000Bq/ml		
1 Bed 30 min	mean activity conc. (Bq/ml)	volume (litres)	Total Activity (MBq)	Deviation
True activity 1211 MBq	845509	1.73	1460	20.6%
Normal Bed				
2 Beds a´ 30 min	mean activity conc. (Bq/ml)	volume (litres)	Total Activity (MBq)	diff (%)
True activity 1198 MBq	794232	1.73	1373	14.6%
Min Bed				
2 Beds a´ 30 min	mean activity conc. (Bq/ml)	volume (litres)	Total Activity (MBq)	diff (%)
True activity 1182 MBq	802365	1.76	1415	19.7%
Max Bed				
2 Beds a´ 30 min	mean activity conc. (Bq/ml)	volume (litres)	Total Activity (MBq)	diff (%)
True activity 982 MBq	722963	1.55	1124	14.5%

Table 14. Specified results from the SPECT measurement with the "liver" volume in the water phantom.

SPECT			
# iterations	Measured activity (MBq)	True activity (MBq)	Deviation
3	1490	1227	+21.4%
10	1533	1227	+24.9%
20	1544	1227	+25.8%
50	1553	1227	+26.6%
100	1559	1227	+ 27.0%

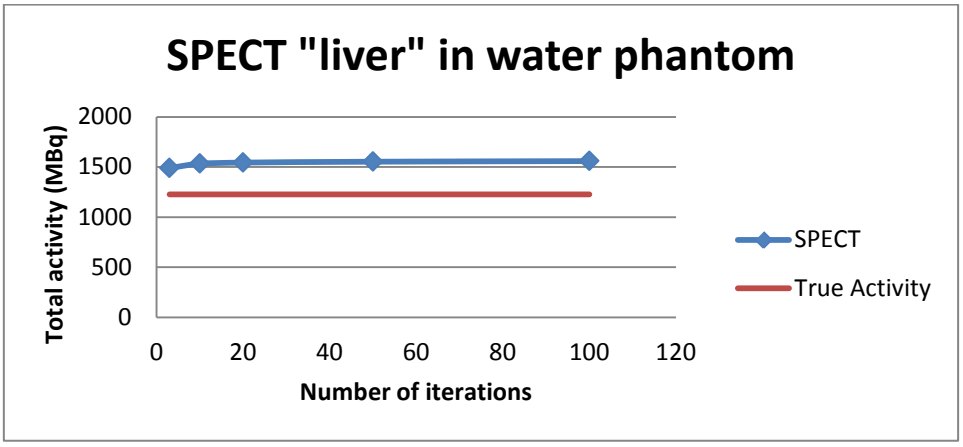

Figure 37. Results from the SPECT measurement with the "liver" volume in the water phantom.

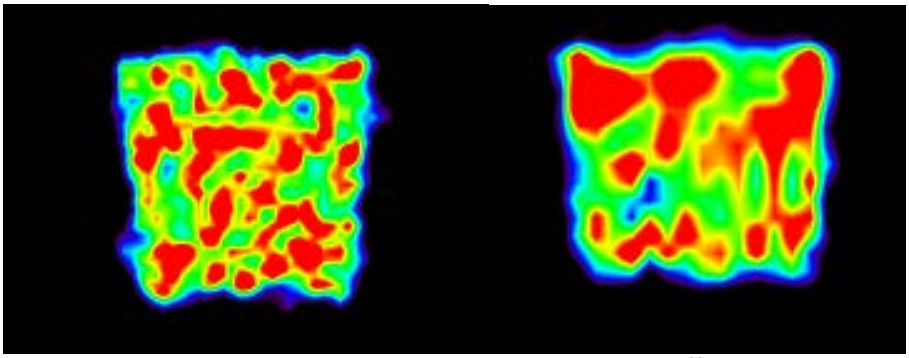

Figure 38. PET-images from the simulated "liver" with ^{90}Y (3) to the left and SPECT image to the right.

Both the PET and SPECT image, shown in Figure 38 is visually almost equal, but there is difference in the quantitative values. The activity distribution is rather homogenous, as seen, but the results here shows that the quantitative activity from the SPECT camera is overestimated. The reason for this is not yet determined, but one reason could be that this measurement contained a source of high ^{90}Y activity as compared to the other phantom setups and also when comparing to the patient activities.

Conclusion

When comparing SPECT with PET the result in this work shows that the PET have the potentials of being superior to SPECT. Even though the SPECT system produced the best numerous quantitative results, the PET activity quantification result might be improved if an appropriate background noise reduction method can be developed and applied. The errors associated with internal dosimetry are of the same order as the results from SPECT and PET measurements.

Measuring the background noise, coming from prompt gammas within the LYSO crystal (as shown in Figure 16), will provide a hint of the magnitude of the quantitative error. The spatial position of the events will be randomly distributed and thus not be localized at the same position during a specific measurement. Thus a background image cannot be applied for a simple subtraction. A compensation for these unwanted hotspots is of course necessary for accurate activity quantification or else voxels will get a larger quantitative result, thus leading to an apparent larger activity. If knowledge about the location of the voxels that is most affected by this additional background noise could be determined, then a spatial dependent correction factor could be determined. Since this has not been the case, the overestimation may be 15% each, or 100% for a smaller number of voxels.

When measuring ^{90}Y with a PET camera system sensitivity of about 5 cps/MBq, it is not unlikely that a contribution of counts coming from the radioactivity in the LYSO crystals that is in the order of 1cps, according to Bettinardi et. al, may have an impact on the results [22]. But if all of the additional 20% activity from the PET patient measurements is caused by this is not clear. It is somewhat tempting to say that a subtraction of 20% from the PET image would be a sufficient accurate result.

The results from the SPECT study do not show the same consistency and thus seem to vary between different activity levels. More measurements would therefore be necessary to verify this assumption. The results indicate that high count rate level may overestimate the activity and that at low count rates the activity seems to be underestimated.

On the other hand, the PET camera seems to gain from a larger ^{90}Y activity since the results are somewhat improved, as shown in Table 13, compared to the patient results. Even though it is of the order of 5% difference it could most likely be traced to the larger ^{90}Y activity and thus the better statistics in the image. Also the PET-system seems more stable with varying activity levels, almost stable with an overestimation of 20 percent, most likely due to a necessary background noise subtraction from the LYSO crystal elements. Once again, more experiments and evaluations would be required to verify these assumptions.

Acknowledgements

I would like to say thank you to some people who has helped me through this master project.
First of all, thanks to Michael Ljungberg and Cecilia Hindorf for great support through this project.
Thanks to Mikael Peterson and Jenny Oddstig for creative inputs when I needed them.
Thanks to all kind staff at the department of clinical physiology and nuclear medicine at the Skåne University Hospital in Lund.

And also, thanks to my wonderful classmates trough the last five years.

References

1. Lhommel, R., et al., *Yttrium-90 TOF PET scan demonstrates high-resolution biodistribution after liver SIRT.* Eur J Nucl Med Mol Imaging, 2009. **36**(10): p. 1696.
2. Lhommel, R., et al., *Feasibility of 90Y TOF PET-based dosimetry in liver metastasis therapy using SIR-Spheres.* Eur J Nucl Med Mol Imaging, 2010. **37**(9): p. 1654-62.
3. Nickles, R.J., et al., *Assaying and PET Imaging of Yttrium-90:1>>34ppm>0.* IEEE Nuclear Science Symposium Conference Record, 2004. **6**: p. 3412-14.
4. Greenberg, J.S. and M. Deutsch, *Positrons from the Decay of P^{32} and Y^{90}.* Physical Review, 1956. **102**(2): p. 415-421.
5. ENSDF, *ENSDF Decay Data in the MIRD Format*, 1998.
6. NIST. *estar stopping power and range tables for electrons*. 2012; Available from: http://physics.nist.gov/PhysRefData/Star/Text/ESTAR.html.
7. Minarik, D., *Activity quantification based on bremsstrahlung scintillation camera imaging for absorbed dose assessment*, in *Department of Medical Radiation Physics*2010, Lund: Lund, Sweden. p. 53.
8. Giammarile, F., et al., *EANM procedure guideline for the treatment of liver cancer and liver metastases with intra-arterial radioactive compounds.* Eur J Nucl Med Mol Imaging, 2011. **38**(7): p. 1393-1406.
9. Läkemedelsverket, *TechneScan LyoMAA kit radio prep*, Läkemedelsverket, Editor 2012, Läkemedelsverket.
10. Murthy, R., et al., *Yttrium-90 microsphere therapy for hepatic malignancy: devices, indications, technical considerations, and potential complications.* Radiographics, 2005. **25 Suppl 1**: p. S41-55.
11. Kennedy, A., et al., *Recommendations for radioembolization of hepatic malignancies using yttrium-90 microsphere brachytherapy: a consensus panel report from the radioembolization brachytherapy oncology consortium.* International journal of radiation oncology, biology, physics, 2007. **68**: p. 13-23.
12. Peterson, M., *SOP Administreringsprotoll 99m-Tc-LyoMAA för SIRT*, 2011: Skånes Universitetssjukhus Lund.
13. Gates, V.L., et al., *Internal pair production of 90Y permits hepatic localization of microspheres using routine PET: proof of concept.* J Nucl Med, 2011. **52**(1): p. 72-6.
14. Minarik, D., K. Sjogreen Gleisner, and M. Ljungberg, *Evaluation of quantitative (90)Y SPECT based on experimental phantom studies.* Phys Med Biol, 2008. **53**(20): p. 5689-703.
15. Healthcare, G., *Discovery PET/CT 690* in *LightSpeed VCT Datasheet*2009. p. 1-22.
16. Healthcare, G., *Discovery PET/CT 690*, 2010.
17. Saha, G.B., *Basics of PET imaging : physics, chemistry, and regulations*. 2nd ed2010, New York: Springer. xiv, 241 p.
18. Valk, P.E., *Positron emission tomography : basic science and clinical practice*2003, London ; New York: Springer. xix, 884 p.
19. Khalil, M.M., *Basic sciences of nuclear medicine*2010, New York: Springer.
20. Healthcare, G., *Clinical implementation of VUE Point FX™*, 2009.
21. Wollenweber, S.D., D.L. McDaniel, and C.W. Stearns, *Method and system for scatter correction*, 2011, General Electric company. Schenectady, NY (US): US.

22. Bettinardi, V., et al., *Physical performance of the new hybrid PETCT Discovery-690.* Med Phys, 2011. **38**(10): p. 5394-411.
23. Kennedy, A.S., et al., *Resin 90Y-microsphere brachytherapy for unresectable colorectal liver metastases: modern USA experience.* Int J Radiat Oncol Biol Phys, 2006. **65**(2): p. 412-25.
24. Knoop, B.O., et al., *Use of recovery coefficients as a test of system linearity of response in positron emission tomography (PET).* Phys Med Biol, 2002. **47**(8): p. 1237-54.
25. Boellaard, R., et al., *The Netherlands protocol for standardisation and quantification of FDG whole body PET studies in multi-centre trials.* Eur J Nucl Med Mol Imaging, 2008. **35**(12): p. 2320-33.
26. Prešnajderová, E., P. Prešnajder, and P. Povinec, *Comment on internal pair production in nuclear decay.* Zeitschrift für Physik. A. Atoms and nuclei, 1979. **291**(3): p. 283-285.
27. Soret, M., S.L. Bacharach, and I. Buvat, *Partial-volume effect in PET tumor imaging.* J Nucl Med, 2007. **48**(6): p. 932-45.
28. Sydoff, M., et al., *Absolute quantification of activity content from PET images using the Philips Gemini TF PET/CT system.* Radiat Prot Dosimetry, 2010. **139**(1-3): p. 236-9.
29. Geworski, L., et al., *Recovery correction for quantitation in emission tomography: a feasibility study.* Eur J Nucl Med, 2000. **27**(2): p. 161-9.
30. Association, N.E.M.A., *NEMA NU 2*, in *Performance measurment of positron emission tomographs*2001. p. 7-10.